DOE/PC/91293--T5

DIRECT CATALYTIC DECOMPOSITION OF NITRIC OXIDE

Maria Flytzani-Stephanopoulos
Adel F. Sarofim
Yanping Zhang

Final Report
June 15, 1995

Prepared for :
U.S. Department of Energy
Pittsburgh Energy Technology Center
Pittsburgh, Pennsylvania
Technical Project Officer - Dr. K. Das (DOE/METC)
Grant Number DE-FG22-91PC~~91923~~ 91293

By
Massachusetts Institute of Technology
Department of Chemical Engineering
Cambridge, Massachusetts

Direct Catalytic Decomposition of Nitric Oxide

Yanping Zhang, Maria Flytzani-Stephanopoulos,[a] and Adel F. Sarofim

Department of Chemical Engineering, Massachusetts Institute of Technology
Cambridge, MA 02139

Abstract

This project investigated a suitable catalyst system for the direct NO decomposition for post-combustion NO_X control. The studied process does not use a reductant, such as ammonia in the case of Selective Catalytic Reduction (SCR) process for catalytic reduction of NO_X to nitrogen.

This is a simplified process basically involving passing the flue gas through a catalytic converter, thus avoiding problems generally associated with the commercial SCR process, namely high operating cost, ammonia slip, and potential N_2O emissions. The main results from this research project are summarized in the following:

Cu-ZSM-5 and M/Cu-ZSM-5 were synthesized by incorporating metal cations into ZSM-5 zeolite supports by optimized ion exchange procedures. It was found that (1) the catalytic activity of Cu-ZSM-5 only increased with copper loading when the Cu-ZSM-5 was prepared in an aqueous copper acetate solution with pH lower than 5.74; (2) high pH of the solution led not only to ion-exchanged Cu^{2+}, but also copper deposition on the zeolite surface forming inactive CuO particles as identified by STEM/EDX and XRD; (3) the sequence of metal ion exchange first, followed by copper ion exchange to synthesize M/Cu-ZSM-5, where M represents any metal ion but copper, was important for the cocation to show promotion effects; and (4) air-calcination of M-ZSM was effective in keeping M cations in the zeolite during subsequent copper ion exchange.

Positive alkaline and rare earth metal cocation effects on the Cu-ZSM-5 were identified in oxygen-containing gas mixtures in the high temperature region (450- 600°C). Cerium ion promoted the Cu-ZSM-5 activity in the low

---

[a] Current Address: Department of Chemical Engineering, Tufts University, Medford, MA 02155.

temperature range (< 450°C) in oxygen-free gas mixture, while alkaline earth and transition metal cocations improved the NO conversion to N_2 in high temperature region.

Cerium modified Cu-ZSM-5 showed higher wet-gas activity for NO decomposition than the Cu-ZSM-5, and also recovered a higher fraction of its initial dry-gas activity after removal of water vapor. It was found that both ion-exchanged cerium as well as cerium oxygen clusters on the zeolite surface are important in improving the Cu-ZSM-5 catalyst performance in water vapor-containing gases. Characterization of fresh and steamed Cu(141)-ZSM-5 and Ce(60)/Cu(138)-ZSM-5 was performed by XRD, STEM/EDX, and XPS. XRD patterns confirmed that cerium ions stabilize the ZSM-5 structure. Uniform Al and Cu distribution, and strong Cu cation association with Al in the freshly calcined Cu(141)-ZSM-5 samples was found by STEM/EDX. The steamed samples, however, showed many copper-containing aggregates, which were identified as CuO by XRD. Based on XPS measurements, it appears that CuO particles are formed inside the zeolite particles. The experimental results showed that Cu-ZSM-5 deactivation by water vapor is primarily due to Cu migration and CuO sintering. However, the effect of water vapor on Cu-ZSM-5 activity is reversible for low water vapor concentration (< 10%) at low temperatures (≤ 400°C). In the Ce/Cu-ZSM-5 system, less extensive CuO formation and copper redistribution were found. It is concluded that Ce cations stabilize Cu in Cu-ZSM-5 by controlling Cu siting and decreasing copper aggregation/sintering.

INTRODUCTION

The removal of nitric oxide from exhaust gas streams in power plants, industrial boilers and engine systems continues to be a challenge in view of new more stringent regulations. A particularly high-priority need is the efficient control of NOx in lean-burn engine exhaust, e.g., gas turbine-exhaust gas, diesel engines, etc. The simplest method for NOx control would be catalytic decomposition to benign N_2 and O_2. Iwamoto and coworkers first reported that Cu^{2+}-ZSM-5 zeolites have stable activity for the direct decomposition of NO even in the presence of oxygen [1]. Subsequently several studies of this catalyst system followed [2-5]. The main problems associated

with further development of the Cu-ZSM-5 catalyst for NO decomposition are reduced activity at high temperature (>500°C), hydrothermal stability problems, and poisoning by SO_2. The latter can be handled in many exhausts by separate removal of SO_2 upstream of the NOx catalyst.

All reports of Cu-ZSM-5 catalyst activity agree that excessively copper ion-exchanged ZSM-5 catalysts give higher N_2 yields [1-3]. Here, "excessively" indicates above the theoretical ion exchange level, corresponding to one divalent Cu^{2+} ion for every two $[AlO_2]^-$ sites in the zeolites. Iwamoto, et. at. [6] reported that it is impossible to prepare excessively copper ion-exchanged zeolites from aqueous solutions of cupric nitrate or sulfate. However, increasing the pH of the solution by addition of basic compounds readily achieved "over-exchanged" copper in ZSM-5 [7]. The copper loading increased with pH from 4 to 9 and reached a nearly constant value above pH = 9. The conversion NO to N_2 over the catalysts with Cu^{2+} exchange from 130- 150% was approximately the same.

It was reported by Kagawa and coworkers [8] that the incorporation of cocations into Cu-ZSM-5 catalysts promoted the high-temperature activity for NO decomposition in O_2-free gas streams. Work in this laboratory has further shown a positive cocation effect on the NO decomposition in both O_2-free and O_2-containing gases with various NO concentrations [9]. For the positive effect to be displayed, it is necessary to follow a specific mode of ion exchange during catalyst preparation.

All NO_x-containing combustion gases also contain significant amounts of water vapor (2- 15%), therefore resistance to water poisoning is important for practical application of a catalyst. Iwamoto, et al [10] and Li and Hall [11] reported that the catalytic activity of Cu-ZSM-5 for NO conversion to N_2 was decreased in the presence of 2% water vapor, but it could be recovered after removal of water vapor. No details about temperature-time effects on wet NO decomposition have been reported.

In the present work, we address issues of Cu-ZSM-5 preparation, and effects of cocations on the catalytic activity of Cu-ZSM-5. Metal modified Cu-ZSM-5 catalysts were tested in both O_2-free and O_2-containing gases, as well as in wet (2- 20% H_2O) gas streams.

EXPERIMENTAL

Catalyst Synthesis and Characterization

(1) Effect of pH on Cu States and Catalytic Activity in ZSM-5

To examine pH effects on the Cu states in ZSM-5 and catalytic activity for NO decomposition, two sets of Cu-ZSM-5 catalysts were prepared.

A first set of catalysts was synthesized by exchanging Cu^{2+} cations into ZSM-5 from dilute aqueous $Cu(ac)_2$ solutions. The parent zeolite was a Na-ZSM-5 (Si/Al = 21.5) zeolite obtained from the Davison Chemical Division of W. R. Grace & Company (SMR 6-2826-1192). The following preparation procedure was used in this work. First, cupric acetate was dissolved in deionized water to form an aqueous solution with a concentration of 0.007 M and initial pH of 5.74. Second, the pH of the solution was adjusted by adding either acetic anhydride or aqueous ammonia into the solution to a desired pH value. The ZSM-5 particles were added into the solution in amounts corresponding to replacing all the Na^+ ions in ZSM-5 by half the number of Cu^{2+} in the cupric acetate solution. The mixture was then vigorously stirred by a magnetic stirrer at room temperature for 19 hours. Finally, the sample was washed with deionized water at room temperature for 30 minutes. After filtration, the samples were dried in air at 100°C overnight. Seven Cu-ZSM-5 catalysts were prepared according to this procedure at pH of 4.5, 4.9, 5.74, 6.0, 6.5, 7.0 and 7.5.

A second set of Cu-ZSM-5 samples with 10- 141% Cu exchange levels were all prepared at pH = 5.74. The procedure was the same as that described above. Low Cu exchange levels were achieved by adjusting the ratio of Cu^{2+} to Na^+ in the slurry. Repeated exchanges were used to increase the Cu exchange level. The highest Cu exchange level, 141%, was obtained after three consecutive exchanges under the conditions described above. The preparation procedures of the two sets of Cu-ZSM-5 catalysts are summarized in Table 1.

(2) Synthesis of Metal Ion Modified Cu-ZSM-5 Catalysts

In catalysts containing copper and a cocation, the ZSM-5 zeolites were first ion-exchanged with the cocation in nitrate form in dilute aqueous solution with concentration of 0.007M. The exchanges were made either at room temperature for 10 hours or at 85°C for 2 hours. After filtration, the metal ion-exchanged ZSM-5 zeolites were dried at 100°C for 10 hours, and some of them were further calcined in a muffle furnace in air at 500°C for 2

hours. The reason for calcining the catalysts was to stabilize cations in the zeolite. The catalysts were further ion-exchanged with Cu^{2+} in an aqueous solution of cupric acetate of concentration 0.007M at room temperature overnight. This was repeated several times, depending on the desired Cu exchange levels. Finally, the catalysts were washed with deionized water at room temperature and dried at 100°C overnight. A catalyst with intermittent air calcination of cocation exchanged ZSM-5 is designated as M/Cu-Z catalyst in the text.

The exchange mode described here was the evolution of several different preparation methods. A summary of observations made during this process when using Mg^{2+} as the cocation is as follows: (1) exchanging copper ions first or co-exchanging copper and magnesium ions for Na^{+} in the ZSM-5 did not achieve high-exchange levels of Mg^{2+} in the zeolite; (2) even when Mg^{2+} was exchanged first followed by copper ion exchange, we would observe loss of Mg^{2+} in the solution. Both (1) and (2) are the result of a more favorable exchange equilibrium for Cu^{2+}/Na^{+} [12]; (3) when the Mg^{2+} ion solution was heated at 85°C for 2 hours, higher levels of exchange were obtained and better stability in subsequent room temperature copper ion exchanges; d) air calcination of Mg^{2+}-exchanged zeolites at 500°C for 2 hours was very effective in keeping the Mg^{2+} exchange high even after subsequent copper ion exchanges. This procedure was followed in preparing two of the Mg/Cu-Z catalysts shown in Table 2. Similarly, Sr, Ni, Pd, Ce and La/Cu-Z prepared with the same technique could retain the cations in the zeolite cavities [9].

(3) Elemental Analysis of Cu-ZSM-5 and M/Cu-ZSM-5

The elemental analyses were performed by Inductively Coupled Plasma Emission Spectrometry (ICP, Perkin-Elmer Plasma 40) after catalyst samples were dissolved in HF(48%), and the solution was diluted to 2% HF by deionized water, while Ce-containing catalysts were dissolved in special solutions purchased from Unisol, Inc. for ICP analyses since Ce^{3+} species are fluoride insoluble. These reagents consist of three types of solutions: UA-4, UNS-2A and UNS-2B. The UA-4, containing HF, dissolves the catalysts, the UNS-2A and UNS-2B neutralize and stabilize the solution to (1) deactivate the HF by increasing the pH to a value of 7.5 to 8.0, and (2) maintain solubility of the samples. Ratios of elements, such as Si, Al, Cu, Na, Mg, Ce, etc. to Al

were calculated based on the elemental contents measured by ICP. In the text, the catalysts are identified in the following ways: (1) Cu(exchange level)-ZSM-5(pH); (2) cocation type(percent exchange level)/Cu(percent exchange level)-Z, for example, Mg(34)/Cu(86)-Z, where 100% ion exchange level is defined as one Cu^{2+} (or Mg^{2+}) replacing two Na^{+} [or neutralizing two $(AlO_2)^{-}$] and the atomic ratio Cu (or Mg)/Al = 0.5.

(4) Characterization of Cu-ZSM-5 and M/Cu-ZSM-5

The catalysts prepared in this study were also characterized by X-ray diffraction (XRD, Rigaku 300) to examine the crystal structures, as well as CuO formation. The samples were evacuated at 55°C for 24 hours, then placed in a dessicator with drying agent. The diffraction patterns were taken in the 2θ range of 5- 80° at a scanning speed of 1° per minute.

Characterization of the Cu-ZSM-5 samples by a state-of-art Scanning Transmission Electron Microscope (VG Microscopes, HB 603 STEM) was also performed to examine Cu distribution in the Cu-ZSM-5 samples. The fresh samples were calcined in a muffle furnace in air at 500°C for 2 hours prior to STEM analysis. The calcined samples were placed on a 200 mesh carbon-covered plain nickel grid for the STEM study. The calcined samples on the grids were coated by carbon in vacuum to further ensure no particle charging during the STEM analysis. The STEM was equipped with a X-ray microanalytical probe, which was used to analyze the composition of catalysts and simultaneously collect energy dispersive data of elements Si, Al, Cu, and Ce with 1.4Å optimum resolution at magnification of 1×10^6. Elemental mapping was performed with this probe on the basis of 128 x 128 data matrix.

X-ray-excited photoelectron spectroscopy (Perkin Elmer, Model 548 ESCA) with 2 mm spatial resolution was used to record XP spectra of the samples. The atomic ratios of copper, cerium, oxygen and silicon on the fresh and used catalyst samples were calculated by using the software supplied with XPS system based on the measured spectra. A Mg$K\alpha$ anode X-ray source (300 W, 15 KV) provides high signal intensity, and 178 eV of a fixed pass energy was used. The base pressure in vacuum chamber was less than 7.5×10^{-8} torr. A layer of catalyst sample in powder form was pressed on a double-sided transfer tape adhered on a 1 in. x 0.5 in. aluminum sheet. The sample was, then, introduced into the XPS vacuum chamber and placed on a sample holder. The total time for acquisition of Cu, Ce, O and Si core level spectra

was 20 minutes after the sample had been exposed to X-ray for 10 minutes. Binding energy was referred to C_{1s} = 284.6 eV. It was found that the C_{1s} line shifted 3.0 eV higher than 284.6 eV owing to sample charging since the catalyst materials were non conductive.

Conversion Measurements and Kinetic Studies

Conversion and kinetic measurements of NO decomposition over Cu-ZSM-5 and M/Cu-ZSM-5 were performed in laboratory-scale packed-bed reactors, consisting of a 60 cm long quartz tube with I.D. equal to 1.1 cm(for conversion measurements) or 0.4 cm (for kinetic studies). A porous quartz fritted disk was placed in the middle of the tube to support the catalyst bed. The reactor was placed in a temperature-programmed furnace that was electrically heated and controlled by a temperature controller (Tetrahedron: Model Wizard). Three mass flow controllers were used to measure flow rates of NO + He, O_2+ He and He. Certified standard helium and gas mixtures were used from Matheson and Airco. A gas chromatograph (Hewlett Packard: Model 5890) with a thermal conductivity detector, and a 5A molecular sieve column of 1/8 in. O.D. by 6 ft. long, was used to measure concentrations of nitrogen, oxygen and nitric oxide. A NO-NOx analyzer (Thermo Electron: Model 14A) was also used to measure low NO/NOx concentrations, ranging from 0.001 ppm to 2,500 ppm. An amount of 0.5-1.0 g of catalyst was placed in the reactor for conversion measurements, and 30-35 mg for kinetic studies. The catalyst packing density in the reactor was about 0.5 g/cc. Total flowrates of the feed gas were 30-90 cc/min. (NTP). The contact time, W/F, defined as the ratio of catalyst weight in the reactor to the total flowrate of the feed gas was 0.03- 1g s/cc(NTP). The total gas pressure in the reactor was 1.5 atm during the conversion measurements and about 2 atm in the kinetic studies. NO concentrations varied from 0.2- 4% in the feed gas stream, O_2 from 0- 5%, balance He. The O_2+ He stream was heated to 150°C before it was mixed with NO + He at the inlet of the reactor to avoid NO_2 formation [9]. All measurements were made after steady state had been reached.

Since typical NOx-containing combustion off-gases also contain a significant amount of water vapor (2-15%), the hydrothermal stability of catalysts was tested in this work. Pure He flowing through deionized water in a constant temperature water saturator was used to entrain water vapor to the

reactor through an electrically heated line. A cold trap (dry ice) was installed at the reactor exit to condense the water vapor prior to analyzing the exhaust gas by GC.

Cocation Effect on the Hydrothermal Stability of Zeolite Structure

Understanding catalyst deactivation due to steaming is one of the importance for application of the these catalysts. However, it is difficult quantitatively to distinguish copper-induced and dealumination-induced catalyst deactivation by using XRD and STEM analyses. The loss of ion exchange capacity of steamed or used catalysts was measured in this work to indicate the extent of dealumination. These tests were conducted as follows: The used catalysts were removed from the reactor, and treated with a solution of 0.05 M HNO_3 for 4 hours to dissolve all the exchanged copper. The catalysts were washed by deionized water, dried in air at 100°C for 10 hours and heated at 500°C for 2 hours. A small amount of the catalyst samples was analyzed by ICP to determine the residual amount of copper. The remaining was ion-exchanged with copper acetate solution thrice, following the procedures described earlier. The catalysts were filtered and dried overnight in air at 100°C, and the amount of re-exchanged copper ion was measured by ICP. Subsequently, the NO conversion to N_2 over the re-exchanged catalysts was measured. The analyses of the catalysts and the conditions of steaming are given in Table 3.

RESULTS AND DISCUSSION

Effect of pH on Cu Loading and Catalytic Activity

(1) Effect of pH on Cu exchange level

The dependence of Cu^{2+} ion-exchange levels on the pH of cupric acetate solution in the first set of Cu-ZSM-5 samples showed the Cu^{2+} exchange level increased with increasing pH, leveled off at about pH = 6.0, then increased further showing a maximum at pH = 7.0 [14]. The results are shown in Figure 1.a. Aluminum was not found by ICP in residual solutions, and no structural change of the zeolite was observed from X-ray diffraction patterns

of the Cu-ZSM-5 samples after the ion exchange, which is in agreement with what has been reported by Iwamoto, et al. [13].

(2) NO conversion to N_2 and O_2

The catalytic activities of the catalysts prepared in this work were evaluated for NO decomposition in a mixture of 2% NO + He at a contact time of 1.0 g s/cc (NTP) and temperature in the range of 350-600°C. Nitric oxide was introduced into the inlet stream after the catalyst was exposed to pure He stream at 500°C for 2 hours at a total pressure of 1.3 atm.

Figure 1.b shows the NO conversion to N_2 over the first set of Cu-ZSM-5 samples. The activity of these catalysts for NO decomposition to N_2 increased with the Cu exchange level when the pH used in preparation was less than 5.74. However, over the catalysts prepared at higher pH with high nominal Cu^{2+} exchange levels, the NO conversion to N_2 curves overlap with that of Cu(102)-ZSM-5(5.7) over the whole temperature range. Here, the catalytic activity no longer increases with the Cu^{2+} exchange level. This suggests that part of the copper contained in the samples is not active for NO decomposition. It is noted that the NO conversion to N_2 over the Cu(96)-ZSM-5(6.0) catalyst was almost 20% lower than that over the Cu(102)-ZSM-5(5.74). This is not the case for two catalysts with similar Cu^{2+} exchange levels (here, 97% and 102%) in the second set of Cu-ZSM-5 samples, both prepared at pH = 5.74 (Table 1 and Figure 2)

In contrast with the first set of samples, the catalytic activities of the second set increased monotonically with the Cu^{2+} exchange level. The NO conversion to N_2 at 500°C over these samples is depicted in Figure 2 as a function of Cu exchange level.

As shown in Figure 1.b, a certain amount of copper ions in the samples prepared at high pH was not active for NO decomposition, since the NO conversion did not increase with copper exchange level. The Cu^{2+} distribution in the catalysts can be evaluated in terms of "surface Cu" and "ion-exchanged Cu" cations. Unlike the first set of samples, Cu^{2+} cations in the second set of Cu-ZSM-5 catalysts were stoichiometrically ion-exchanged with Na^+ ions, approximately, as shown in Table 1, when Cu ion exchange level was lower than about 90%. The correlation of catalytic activity with the amount of ion-exchanged Cu, as shown in Figure 2, can be used as a standard to determine how much copper ion was "ion-exchanged" in each of the first

set of the Cu-ZSM-5 catalysts. The difference between the total Cu and "ion-exchanged Cu" is, here, designated as "surface Cu", which is not active for NO decomposition. The Cu distribution in the first set of samples is shown in Figure 3.

We have studied the contribution of the "surface Cu" and "ion-exchanged Cu" to the catalytic activity [14]. It was found that the "surface Cu" could be easily removed by aqueous ammonia, and was inactive for NO decomposition.

(3) Characterization of catalysts by STEM/EDX and XRD

Figure 4 shows a STEM micrograph of the 500°C, 2h-calcined Cu(165)-ZSM-5(7.0) sample. This is representative of the catalysts prepared at high pH (> 6.0). The phase contrast imaging demonstrated formation of copper particles (up to 6 nm) clearly distinguishable from the zeolite support. The X-ray spectra of a copper aggregate and the Cu-ZSM-5 background showed a very strong copper signal on the bright spots of the dark field STEM micrograph [14] (Figure 4). Copper X-ray mapping showed homogeneously dispersed copper in the sample, and confirms formation of copper particles on the edges and voids of the zeolite crystal. This can be seen on the X-ray maps of Cu and Si, as shown in Figure 5 (scale of one elemental mapping: 100 nm by 120 nm), for the same area as that in Figure 4.

XRD patterns similar to that of the parent ZSM-5 zeolite were obtained for both sets of Cu-ZSM-5. No other crystalline phase, such as CuO, was found by XRD in the fresh samples. However, CuO could be clearly seen by XRD in samples prepared at high pH after air calcination. An example is shown in Figure 6 for Cu(154)-ZSM-5(7.5) after 2h-air calcination at 500°C. For comparison, Figure 7 shows the XRD pattern of this sample as well as that of the parent ZSM-5 in the range of 2θ = 34- 40° in which CuO has the strongest diffraction peaks.

Nitric Oxide Decomposition over Metal Ion Modified Cu-ZSM-5

(1) Nitric Oxide Decomposition in the Absence of Oxygen

The Cu-ZSM-5 and Mg/Cu-ZSM-5 catalysts shown in Table 2 were evaluated in a gas containing 2% NO- He, at contact time of 1.0 g s/cc (NTP) over the temperature range of 350- 600°C. Control experiments with Mg-ZSM-

5 materials verified that the activity of Mg/Cu-ZSM-5 was exclusively due to Cu ions. Figure 8 is typical of the NO to N_2 conversion profiles obtained for the catalysts tested under these conditions.

For the same copper ion-exchange level (~70%), the Mg(52)/Cu(66)-ZSM-5 catalyst shows a positive effect, i.e., higher NO to N_2 conversion than the Cu(72)-ZSM-5 material, in the high temperature region (450- 600°C), as can be seen in Figure 7. These results are in agreement with the report by Kagawa, et al [8]. While still present, this effect is not as pronounced for Mg/Cu-ZSM-5 catalysts with Cu exchange level higher than about 100%.

Within the group of the Mg/Cu-ZSM-5 catalysts, preparation conditions were important. As mentioned in the previous section, heating of the solution during Mg^{2+}-exchange was necessary in order to retain the Mg ions in the zeolite upon subsequent exchange with copper ion solutions. The effect of intermittent air calcination of Mg-ZSM-5 material at 500°C for two hours on the catalytic activity was also evaluated. The precalcined catalyst, Mg(34)/Cu(86)-ZSM-5, gave higher NO to N_2 conversion over the whole temperature range (350-600°C) than the catalyst Mg(40.4)/Cu(91.2)-ZSM-5 without intermittent air calcination [9].

At the present time, no consensus exists in the literature on the mechanism of NO decomposition over Cu-ZSM-5 catalysts. This makes a mechanistic interpretation of the cocation effects reported here premature. However, the importance of ion exchange sequence and catalyst heat treatment on the NO decomposition activity is worth discussing in terms of active site modification on the basis of available information. In ESR studies, Kucherov, et al [15, 16] have identified two types of isolated Cu^{2+} ions: one in a five-coordinated square pyramidal configuration, the other in a four-coordinated square planar. At low Cu exchange level, the five-coordinated Cu^{2+} ions were preferably formed. Shelef [17] proposed the square planar copper ions as the active sites of Cu-Z for NO decomposition. This explains the negligible activity of Cu-Z catalysts with low Cu ion-exchange level (<40%). To examine the validity of this assumption we have examined the NO conversion to N_2 over various Cu-Z catalysts as a function of the amount of square planar Cu^{2+} ions, calculated from the data given in Kucherov, et al [16] for Cu-Z catalysts prepared from a ZSM-5 zeolite which had a similar ratio of Si/Al = 21 to the ZSM-5 zeolite used in this study. A linear relationship was found [18]. The number of four-coordinated square

planar Cu^{2+} in Cu-Z materials has been reported to decrease at high temperatures [16]. It may be hypothesized that the inert Mg ions stabilize the relative population of square planar Cu^{2+} ions resulting in higher NO conversion to N_2 at high temperatures, as shown in Figure 7. However, a simple correlation is not adequate proof of the hypothesis. Detailed spectroscopic work is necessary for this.

The intermittent calcination effect may be explained by stronger binding of Mg^{2+}-bare ions, formed during calcination from their respective larger hydrated complex ions, to the ZSM-5 framework in the 5- and 6-membered rings. This would effectively keep the active Cu^{2+} in the 10-membered rings, where they are accessible to the reactant gas molecules. Hence, a higher NO conversion to N_2 is expected for the pre-calcined Mg(34)/Cu(86)-ZSM-5 over the non-calcined Mg(52)/Cu(91)-ZSM-5 catalyst. The observed cocation effect in Kagawa, et al [8] and the present work, therefore, may simply be one of stabilization of the copper active sites. To pursue this argument further, the performance of the intermittent calcined M/Cu-ZSM-5 should not be sensitive to the type of cocation chosen. The NO conversion to N_2 was studied over several precalcined M/Cu-ZSM-5 catalysts with similar Cu^{2+} exchange level, where M is a transition metal or alkaline earth ion. Similar catalytic activity was indicated by overlapping conversion profiles [9].

The NO conversion to N_2 over the Ce(11)-, Ce(26)-, and Ce(60)-ZSM-5, Cu(141)-ZSM-5 and Ce(60)/Cu(138)-ZSM-5 catalysts was evaluated under the above conditions, as shown in Figure 8. We have reported that a low Ce^{3+}-modified Cu-ZSM-5 promoted the catalyst activity in the low temperature region (300-450°C) [9]. The catalyst activity for NO decomposition over the Ce(60)/Cu(138)-ZSM-5 is higher than that over the Cu(141)-ZSM-5 in the low temperature region (350-450°C), while Ce(11)/Cu(119)-ZSM-5 displayed a more pronounced positive effect on the catalytic activity in this region [9]. All Ce-ZSM-5 materials had negligible activity for NO decomposition.

The dry gas-conversion of NO to N2, 92% and 91%, respectively, for Cu(141)-ZSM-5 and Ce(60)/Cu(138)-ZSM-5 at 500°C is used as the basis to calculate relative NO conversion to N2 in wet gas conditions.

(2) NO decomposition in O_2-containing gases

Oxygen has been reported to inhibit the NO decomposition reaction, but the inhibition decreases with temperature [19]. The oxygen effect was studied

on Cu-ZSM-5 catalysts using high NO concentrations (1-4%) in the feed gas. Iwamoto, et al [10] have reported that in oxygen-containing gas the NO conversion to N_2 does not decrease as much for over-exchanged Cu-ZSM-5 catalysts. However, a large decrease was shown for low Cu ion-exchanged Cu-ZSM-5.

In the present work we examined the effect of oxygen on the catalytic activities of both the Cu-ZSM-5 and cocation-exchanged M/Cu-ZSM-5 catalysts. Figure 9 shows typical conversion- temperature plots for the Cu (141)-ZSM-5 catalyst with 0 and 5% O_2 containing gases with NO content fixed at either 2% or 0.2%, W/F = 1 g s/cc (NTP). The data display the O_2-inhibition and the lower-sensitivity to O_2 at high temperature as mentioned above. However, it is very interesting that a similar plot for low NO-content (0.2%) in the gas (Figure 9), shows much less inhibition by oxygen at low temperatures and no oxygen-effect in the high-temperature region. Figure 10 shows effects of oxygen on NO decomposition to N_2 over the Cu(97)-ZSM-5 catalyst in 2% NO- He. Similar trends are observed as for Cu(141)-ZSM-5.

Similar experiments were run with the Mg/Cu-ZSM-5 catalysts. Typical results are shown in Figure 10 for the Mg (34)/Cu (86)-ZSM-5 material. In the absence of oxygen the NO conversion over Mg(34)/Cu(86)-ZSM-5 was slightly higher than over Cu(97)-ZSM-5. However, a pronounced positive effect was clear when oxygen was present in the feed gas stream. This is shown in Figure 10 for a gas mixture containing 5% O_2. For the Ce(60)/Cu(138)-ZSM-5 catalyst, a positive effect in the presence of oxygen was also observed as shown in Figure 8.

(3) Kinetic studies of Cu-ZSM-5 and M/Cu-ZSM-5

The microcatalytic reactor described earlier was used with samples weighing 30 mg for kinetic studies and measurements of turnover frequencies over the Cu (72)-ZSM-5, the Mg (52)/Cu(66)-ZSM-5 catalysts. Conversion-contact time plots, constructed for the NO decomposition reaction over each catalyst at 500°C with 4% NO- He gas, were linear for conversions up to 30% for the Mg(52)/Cu(66)-ZSM-5 and 40% for Cu(72)-ZSM-5. In the kinetic studies the conversions were kept lower than 30% to ensure that reaction rates were not diffusion- limited.

The turnover frequencies of NO decomposition over the Cu(72)-ZSM-5 and Mg(52)/Cu(66)-ZSM-5 are shown in Figure 11 in the form of Arrhenius-

plots. Here, the turnover frequency, TOF, is defined as number of NO molecules to N_2 per Cu per second. The turnover frequencies over the Cu(72)-ZSM-5 are higher than for the Mg(52)/Cu(66)-ZSM-5 catalyst over the low temperature range and lower at high temperatures in agreement with the conversion-temperature plot of Figure 7. In this research, the measurements of the TOF were extended to higher temperatures to measure the corresponding apparent activation energy. As can seen in Figure 11, the apparent activation energy for NO decomposition over the Mg(52)/Cu(66)-ZSM-5 is 18.4 Kcal/mole in the low temperature region, changing over to a negative value of -7.9 Kcal/mole in the high temperature region (> 500°C). Over the Cu(72)-ZSM-5 material, similar values of the apparent activation energies, 15.4 Kcal/mole for the low temperature region and -10.1 Kcal/mole for the high temperature region, were obtained. A changing reaction mechanism or loss of active copper coordination at high temperature may explain the observed reaction rate maximum.

For the determination of reaction orders, a power law was assumed. The power law is written as:

$$r = kP_{NO}^{m}P_{O2}^{n}$$

where P_{NO} is the NO partial pressure (pa), $P_{O2}$is the O_2 partial pressure (pa), m was the reaction order with respect to NO and n is reaction order with respect to O_2. Therefore, to determine m, the ln (r) vs ln (P_{NO}) was plotted at each reaction temperature. The slope of the straight line of the ln (r) vs ln (P_{NO}) gives the reaction order m. The concentration of NO was varied in the feed gas stream while keeping the total flow rate constant and oxygen-free. Similarly, the reaction order, n, for O_2 was obtained from the slope of the straight line of the ln (r) vs ln (P_{O2}) at each reaction temperature while P_{NO} and the total flow rate were kept constant.

The dependence of the NO decomposition rate on the partial pressures of nitric oxide and oxygen was investigated over the Cu(72)-ZSM-5 and Mg(52)/Cu(66)-ZSM-5 catalysts at different reaction temperatures. The NO concentration varied from 0.5 to 4%, and O_2 from 1 to 5%. The reaction rate was first order in partial pressure of nitric oxide over Cu(72)-ZSM-5 in the temperature range of 400 to 600°C, as shown in Figure 12a. However, Figure 12b shows the reaction order for NO over Mg(52)/Cu(66)-ZSM-5 being temperature dependent, first order at 400°C and 1.4 at 600°C. The reaction

orders for O_2, as shown in Figure 13 and 14, over Cu(72)-ZSM-5 and Mg(52)/Cu(66)-ZSM-5 were negative 0.5 and negative 0.3, respectively, and temperature independent. Interestingly, the sensitivity to O_2 decreased from Cu-ZSM-5 to metal modified Cu-ZSM-5. Thus, the kinetics are in good agreement with the observed data, i.e., Mg^{2+} cocations moderate the inhibition of NO decomposition by oxygen, as shown in Figure 10.

Since the power law is the most simplified rate expression, it is needed to study kinetic model in detail.

Cu-ZSM-5 Stabilization by Cocations in Wet NO Decomposition

(1) Cocation effect in wet NO-decomposition

The catalytic activity of Cu-ZSM-5 and Mg/Cu-ZSM-5 catalysts was permanently lost after the catalysts had been exposed to a gas mixture of 20% H_2O- 4%O_2- He at 750°C for 20 hours [20]. The loss of catalytic activity may be attributed to either dealumination of the ZSM-5 materials or deactivation of copper, or both. We have recently reported [21] that steaming Na-ZSM-5 materials in 20% H_2O at temperatures above 600°C leads to partial vitreous glass formation, and dealumination indicated by the appearance of an amorphous background (halo) in the XRD diffraction patterns, zero micropore volume as measured by nitrogen gas adsorption, and greatly reduced ion-exchange uptake capacity. On the other hand, little micropore volume loss and Cu^{2+} uptake capacity loss were found for the 500°C-steamed Na-ZSM-5. This fact suggests that the 500°C-steamed Na-ZSM-5 undergoes less significant structural change, compared with the 600°C-steamed Na-ZSM-5. Therefore, the hydrothermal stability and effect of water vapor on the catalytic activity were examined at 500°C for the Cu-ZSM-5 and metal ion modified Cu-ZSM-5 materials. The loss of activity can then be correlated with the copper in the absence of significant structural modifications of the zeolite at 500°C.

A series of tests was performed in 2% NO- He at contact time of 1g s/cc and 500°C under dry (0% H_2O) as well as wet (20% H_2O) conditions over Cu(141)-ZSM-5 and modified Cu-ZSM-5 catalysts. Figure 15 shows the steady-state NO conversion to N_2 over the catalysts Cu(72)-, Mg (52)/Cu(66)-, Cu(141)-, Ba(5)/Cu(126)-, Y(13)/Cu(135)- and Ce(60)/Cu(138)-ZSM-5 under these conditions. Introduction of water vapor into the reactant gas mixture

after the catalysts had been in dry NO-gas for 4 hours drastically decreased the conversion. The wet-gas activities reached a steady state corresponding to 8% NO conversion to N_2 for all catalysts, except 20% conversion over Ce(60)/Cu(138)-ZSM-5, in two hours.

The activity recovery in dry NO-gas after removal of water vapor is shown in Figure 15. The Mg(52)/Cu(66)-ZSM-5 gradually restored some of its activity to about 45% of its original value. However, no recovery was found for the Cu(72)-ZSM-5 catalyst. For the over-exchanged Cu(141)-ZSM-5, 30% of its original catalytic activity was recovered after removal of water vapor. The cocation (Mg^{2+}, Ba^{2+}, Y^{3+} and Ce^{3+}) modified Cu-ZSM-5 catalysts recovered a larger fraction of their original catalytic activity than Cu(141)-ZSM-5. Among these cations, Ce cations displayed the most pronounced positive effect on the wet gas-Cu^{2+} activity as well as on dry gas-activity recovery (more than 66%). The Ce/Cu-ZSM-5 material was, thus, selected further tested.

The performance of the catalysts Ce(60)/Cu(138)-ZSM-5 and Cu(141)-ZSM-5 was studied in a 2% NO - He stream with varying water vapor contents from 2 to 20% at 500°C. Cyclic activity tests in dry and wet conditions were conducted. The results of dry/wet gas cycles for Cu(141)-ZSM-5 and Ce(60)/Cu(138)-ZSM-5 are shown in Figures 16 and 17, respectively, where the steady state catalytic activities relative to the dry gas activity are shown by the horizontal lines. The catalysts were pretreated in pure He at 500°C for two hours prior to introduction of the reactant stream (2% NO - He) into the reactor for initial dry-gas activity tests. Following this dry-gas test for two hours, the catalysts were exposed to 2% water vapor for 10 hours. After this they were subjected to dry gas for 20 hours. In the following cycles, NO conversion to N_2 was measured under wet (using various water vapor contents in 2% NO - He gas stream) and dry conditions. The transition time in terms of reaching steady catalyst activity from wet/dry or dry/wet-gas conditions was about two hours. It was observed that the catalytic activity is decreased more sharply for the Cu(141)-ZSM-5 than for the Ce(60)/Cu(138)-ZSM-5 with increasing water vapor partial pressure in the reaction streams. The latter catalyst displayed twice as high activity as the former in all wet gas mixtures. These results indicate that Ce^{3+} cations can promote the catalyst activity in wet NO decomposition, and restore the activity to a larger extent after removal of water vapor from the gas stream. It is worth pointing out

here that the dry-gas catalytic activities over the steamed catalysts were not affected by treating the samples in pure He at high temperatures (600- 750°C).

The wet (20% H_2O) NO decomposition activity was lower at 600°C than at 500°C for both types of catalysts. Structural changes, such as vitreous glass formation and loss of framework aluminum, are rapid at 600°C in 20% H_2O-gas mixtures [21]. This will result in loss of copper active sites. These effects are irreversible. Heat treatment under dry conditions at 500- 750°C did not restore the catalyst activity after the Cu-ZSM-5 catalysts were deactivated by water vapor [21].

The effect of water vapor on the catalytic activities of the Cu(141)-ZSM-5 and Ce(60)/Cu(138)-ZSM-5 was further evaluated during and after steaming at 400°C (other experimental conditions were the same as those shown in Figure 15). It was found that the permanent loss of catalytic activity after steaming was less than that after 500°C-steaming. The rate of catalytic activity recovery of the Ce(60)/Cu(138)-ZSM-5 was more rapidly than that of the Cu(141)-ZSM-5. The results are shown in Figure 18.

The catalytic activity of the Cu(141)-ZSM-5 was further evaluated in 5% H_2O- 2% NO- He at 400°C for 78 hours. It was interesting to find out that the wet-gas activity was constant for this length of time. After the water vapor had been removed from the reaction stream, about 84% of the dry-gas activity was recovered at 400°C. When the reaction temperature was raised to 500°C, the dry-gas catalytic activity was almost fully restored. Figure 19 shows the above results.

Catalyst characterizations by XRD, STEM/EDX and XPS were performed to examine physical and chemical changes of the fresh and catalytically used Cu(141)-ZSM-5 and Ce(60)/Cu(138)-ZSM-5 samples. Fresh, 100°C-dried samples are referred to as-synthesized. Air-calcined samples were prepared by calcining the as-synthesized samples in air at 500°C for 2 hours. For the catalysts used in dry- and wet-gas streams, there are three kinds treatments: (1) in He for 2 hours, then in 2% NO - He at 500°C for hours; (2) in 20% H_2O - 2% NO - He at 500°C for 10 hours following the first treatment; (3) in 2% NO - He at 500°C for 20 hours following treatment-2 (refer to Figure 15).

(2) Micropore volume measurements

The micropore volumes of the fresh and catalytically used samples were measured by n-hexane adsorption to examine the effect of water vapor on the

catalyst structure. The results are listed in Table 4. After catalytic reaction in 20% H_2O- 2% NO- He at 500°C (or treatment two), the micropore volume loss of Cu(141)-ZSM-5 and Ce(60)/Cu(138)-ZSM-5 was 19% and 15%, respectively. Micropore volume loss is attributed to amorphous material formation, which blocks zeolite channels. The experimental results suggest that Ce cations stabilize the crystal structure and increase its tolerance to water vapor. In wet NO-decomposition at 600°C, the Ce(60)/Cu(138)-ZSM-5 catalyst lost its activity almost completely, and simultaneously lost 32% of its micropore volume.

(3) X-Ray diffraction patterns

XRD analysis of the fresh and used Cu(141)-ZSM-5 and Ce(60)/Cu(138)-ZSM-5 catalysts after the treatment three showed no significant loss of crystallinity for the steamed samples. After steaming the Na-ZSM-5 material, however, at 600°C, vitreous glass formation is indicated by the appearance of an amorphous background (halo) on the diffraction pattern at 2θ = 10- 40°. The steamed Ce(60)/Cu(138)-ZSM-5 in 20% H_2O-2% NO- He at 600°C shows less vitreous glass formation than the steamed Na-ZSM-5 under same treatment conditions, as shown in Figure 20. Its dry-gas activity after the removal of the water vapor is higher than that of Cu(20)-ZSM-5 prepared from the 600°C-steamed Na-ZSM-5 [21]. These results suggest that the presence of Ce and Cu cations in ZSM-5 zeolite stabilizes the crystal structure. Using ^{27}Al-NMR, Grinsted, et al [22] observed aluminum stabilization in H-ZSM-5 by Cu cations after the sample had been exposed to a 10% H_2O-containing gas at 410°C for 113 hours. Effects of cocations on the hydrothermal stability of the zeolite structure are discussed below.

CuO formation is an indication of catalyst deactivation. The XRD patterns of the fresh 500°C-air calcined Cu(141)-ZSM-5 and Ce(60)/Cu(138)-ZSM-5 samples as well as the parent Na-ZSM-5 in the range of 2θ = 34- 40° in which CuO crystal has the strongest diffraction peak showed no CuO phase present in the samples. However, Figure 21 shows CuO formation for the 500°C-steamed Cu(141)-ZSM-5. On the other hand, CuO formation was not observed from the XRD-pattern of the 500°C-steamed Ce(60)/Cu(138)-ZSM-5 which retained 67% of the original dry-gas activity. No other crystalline phases involving copper or cerium were identified by XRD in these samples.

XRD analysis of the highly siliceous ZSM-5 in powder form cannot be used to determine whether the zeolite is dealuminated or not, since removal

of several aluminum atoms (here 4.7 per unit cell) from a unit cell that contains at least 288 atoms does not change the structural factors significantly.

(4) Characterization of samples by STEM/EDX

STEM/EDX mappings (scale of a mapping: 100 nm by 120 nm) of Al and Cu, for the Cu(141)-ZSM-5 in the fresh, 500°C-calcined state and after 10 hour wet- and 20 hour dry-NO decomposition, are shown in Figure 22. Very uniform Al and Cu distribution, and strong Cu cation association with Al on the freshly calcined Cu(141)-ZSM-5 samples are found, Figure 22a (the Al mapping is on the upper left corner, the Cu mapping is on the upper right corner, and an overlapping of the Al and Cu mappings is on the lower left corner). The 500°C-steamed Cu(141)-ZSM-5 catalyst, however, shows many CuO particles, Figure 22b, with mean aggregate sizes of 3-5 nm as estimated from the electron micrographs. It is very interesting to see formation of aluminum aggregates which indicate partial dealumination of the zeolite substrates. It is well known that dealumination leads to the loss of $(AlO_2)^-$ from the zeolite framework, and this can cause a change of coordination and/or easier migration of Cu^{2+} cations. It is not clear what the first step is under these conditions. Cu migration and zeolite dealumination leading to copper aggregation cause loss of catalytic activity.

CuO particles in the Cu-ZSM-5 crystal were also observed by Kharas, et al [23], after Cu(207)-ZSM-5, prepared from an ion-exchange solution of pH = 7.5, was tested in a simulated lean-burn gas mixture in the temperature range of 600-800°C. However, the CuO particles observed by these authors may not be exclusively attributed to copper sintering. As we discussed earlier, CuO particles with a mean size of 5 nm were found to form on the surface of fresh Cu(165)-ZSM-5 calcined in air at 500°C for 2 hours after ion-exchange preparation in a cupric acetate solution of pH = 7.0 and dried in a muffle furnace in air at 100°C overnight. This CuO particle formation is due to Cu(OH)x precipitation on the zeolite in high pH (>6.0) solutions.

Three samples of Ce(60)/Cu(138)-ZSM-5 were examined by using STEM/EDX mapping: sample 1 is fresh, 500°C air-calcined material, sample 2 reacted in the gas stream under the conditions of treatment two, and sample 3 reacted under the conditions of treatment three (refer to Figure 15). As shown in Figure 23a, Cu, Al and Ce are uniformly distributed in sample 1 except for one Ce/Cu aggregate on the right hand-side of the crystal. However, Cu in

sample 2 is enriched on the edges of the catalyst crystal, as shown in Figure 23b. Unlike the catalytically used Cu(141)-ZSM-5 shown in Figure 22b, no apparent Al aggregates were found in sample 2. After removal of water vapor from the reactant gas stream, the Cu cations redistribute in the Ce(60)/Cu(138)-ZSM-5 samples, which leads to the high catalyst activity recovery. The mapping for sample 3 is shown in Figure 23c. From comparison of the copper distribution in sample 3 with that in the fresh Cu(141)-ZSM-5 and Ce(60)/Cu(138)-ZSM-5, it was found that the redistributed Cu did not reach the same uniform dispersion as that in the fresh samples. Therefore, 100% recovery could not be achieved after the wet NO decomposition conditions employed in these tests.

(5) Dynamic change of copper in Cu-ZSM-5 and Ce/Cu-ZSM-5

The atomic surface ratios of copper, cerium, and oxygen to silicon in the fresh and reacted Cu(141)-ZSM-5 and Ce(60)/Cu(138)-ZSM-5 samples were measured by XPS. Atomic ratios of copper, cerium, and oxygen to silicon are shown in Figures 24- 26 for both Cu(141)-ZSM-5 and Ce(60)/Cu(138)-ZSM-5 catalysts after various treatments. Bulk Cu/Si ratio measured from ICP is equal to 0.035 for both the Cu-ZSM-5 and Ce(60)/Cu(138)-ZSM-5, and bulk Ce/Si is equal to 0.01 for the Ce(60)/Cu(138)-ZSM-5. The O/Si of the as-received Na-ZSM-5 equals 2.72. The O/Si ratios, as shown in Figure 24, of the as-synthesized, treated-1, -2, and -3 samples of each catalyst are approximately constant, and a little higher than 2.72 of Na-ZSM-5, implying coverage of the zeolitic crystal by cations.

A picture of copper change in the Ce(60)/Cu(138)-ZSM-5 under different treatments is shown in Figure 25. The surface Cu/Si (= 0.395) of the as-synthesized sample is much higher than the bulk concentration (Cu/Si = 0.035). After treatment-1, copper migrates into the zeolite channels leading to lower Cu/Si, from 0.395 of the as-received to 0.071. Copper migration into ZSM-5 has been recently reported by Shpiro, et al. [24] after heat treatment in oxygen, and nitric oxide. However, it was observed by Haack and Shelef [25] that copper migrated out to the crystal surface region after heat treatment at 500°C in oxygen, and argon. In Cu-Y zeolites, copper has much less mobility [26] than in Ce/Cu-ZSM-5. When water vapor was present in the reactant stream, i.e., under treatment-2, copper migrated out leading to copper enrichment in the surface regions of catalyst particles. It is very interesting to

see that some surface copper moved back inside the zeolite channels under treatment-3, which implied copper redistribution. These results are in good agreement with those observed by copper X-ray mapping by STEM/EDX. However, cerium ions were not as mobile as copper ions as indicated by the fact that Ce concentration on the surface regions only slightly decreases under treatments-2 and -3, compared with that of the as-synthesized sample. It is noted that the surface cerium concentration was much higher than the bulk value in each case, indicating a large amount of cerium oxide clusters on the surface These results are shown in Figure 26.

Copper showed less mobility in Cu(141)-ZSM-5 than in the Ce(60)/Cu(138)-ZSM-5 sample under the same treatments, as shown in Figure 25. The as synthesized sample has higher surface copper concentration (Cu/Si = 0.088) than the bulk (0.035). After treatment-1, copper also migrated into ZSM-5 zeolite resulting in a value of 0.034 for the surface Cu/Si, equal to the bulk value. The Cu/Si increased to 0.06 after treatment-2, and decreased after water vapor was removed from the reaction stream (treatment-3).

(6) Effect of Steaming on Cation Exchange Sites of ZSM-5

Part of catalyst activity of Cu-ZSM-5 and Ce/Cu-ZSM-5 catalysts was permanently lost after steaming at 500 and 600°C. The permanent loss of catalytic activity is attributed to isolated copper loss by aggregation and dealumination as indicated by the XRD and STEM/EDX analysis. Effect of steaming on cation exchange sites of ZSM-5 was examined by the uptake capacity of re-exchanged copper ions and the catalytic activity of the resulting Cu-ZSM-5 .

The ICP results shown in Table 3 give the amount of copper that can be re-exchanged into the steamed materials after removal of copper from the deactivated catalysts. The re-exchanged amount of Cu can be correlated to the structural change of these catalysts. For the Cu(141)-ZSM-5 samples after wet NO decomposition at 500 and 600°C, the re-exchanged copper ion capacities were Cu/Al = 0.47 and 0.27 respectively. The latter is higher than the Cu/Al

value of 0.1 for the 600°C-steamed Na-ZSM-5. Thus, Cu ion-exchanged ZSM-5 has more cation exchange sites than Na-ZSM-5. The Ce(40)/Cu(135)-ZSM-5 samples after wet NO decomposition at 500 and 600°C showed higher copper re-exchange capacities with Cu/Al values of 0.60 and 0.35, which means more cation exchange sites present in the steamed Ce(40)/Cu(135)-ZSM-5 materials.

In a separate control experiment, Ce(60)-ZSM-5 was treated under a similar wet NO decomposition condition at 600°C. The steamed sample had medium-high copper ion exchange capacity with Cu/Al = 0.41 (Table 3). This shows that the steamed cerium ion-exchanged ZSM-5 had also more copper ion exchange sites than the 600°C-steamed Na-ZSM-5.

Catalytic activities of the copper re-exchanged ZSM-5 materials prepared from the steamed catalysts as well as the Cu-ZSM-5 synthesized from the 600°C-steamed Ce(60)-ZSM-5 were evaluated in 2% NO - He at 500°C and W/F = 1.0 g s/cm^3. However, it was found that not all re-exchanged copper ions were active for NO decomposition. The NO conversion over the Cu re-exchanged materials are compared with those over their parent steamed catalysts, and fresh Cu-ZSM-5 prepared directly from the parent Na-ZSM-5 in Table 5.

Obviously, not all Cu ions in the copper re-exchanged ZSM-5 catalysts are active for NO decomposition, compared with the fresh Cu-ZSM-5 materials. Thus, the steamed material contains negatively charged sites which have copper uptake capacity, but, are inactive for NO decomposition, were formed during steaming. Cu deposition on the zeolite surfaces can be ruled out since the color of the used materials remained light blue, and no CuO was detected by XRD. It is interesting that Ce-containing materials created more inactive sites in the steamed catalysts.

The residual catalytic activity of the Cu(141)-ZSM-5 after 500°C-steaming was the same as that of the Cu(94)-ZSM-5 resulted from re-exchanging the 500°C-steamed Cu(141)-ZSM-5 sample (Table 5). This implies that the active sites were not affected by the process of room temperature washing with the 0.005M HNO_3 solution for 4 hours. This is in good agreement with that for the parent Na-ZSM-5-washing with a similar solution. However, the Cu re-exchange ZSM-5 catalyst prepared from the 500°C-steamed Ce(40)/Cu(135)-ZSM-5 showed lower catalytic activity than the original steamed materials. This suggests that there exists a type of active Cu-...Ce-...Al site for NO decomposition, which can be removed by the dilute HNO_3 solution. However, these sites are different from these of the parent Na-ZSM-5 in their ability to resist acid attack. Therefore, the presence of cerium ions serves to stabilize active Cu sites in wet NO decomposition.

The 600°C-steamed samples showed similar performance to the 500°C-steamed samples, except they had even lower Cu ion re-exchange capacity and activity (Table 5).

(7) Change in the active copper sites

NO conversions to N2 over Cu(141)-ZSM-5 and Ce(60)/Cu(138)-ZSM-5 catalysts as shown in Figures 16 and 17 display a dynamic change in the number of active copper sites as indicated by changes in the catalytic activity during the reaction cycles. The number of active copper sites decreases upon introduction of water vapor into the reactant stream, levels off in wet-gas stream 2 hours later, then is partially restored after the removal of the water vapor. We may, therefore, distinguish three types of copper sites: active in wet gas stream, inactive (permanent copper deactivation due to water vapor) in dry gas, and reversibly active sites (recovering activity after removal of the water vapor). The dry-gas NO conversion to N2 over Cu-ZSM-5 catalysts was correlated to Cu ion-exchange levels in a mixture of 2% NO-He at W/F = 1.0 g s/cc (NTP) and 500°C, as shown in Figure 3. This correlation was used to calculate how much ion-exchanged Cu corresponded to the NO conversion

measured in this study. Figures 27 and 28 show the distribution of the three types of copper in the steamed Cu(141)- and Ce(60)/Cu(138)-ZSM-5 under various conditions.

(8) Copper deactivation

The mechanism of Y-zeolite dealumination induced by steaming has been discussed by Kerr [29, 30] and McNicol and Pott [31]. The scheme of the zeolite dealumination in this study is considered to be similar to that of the Y-zeolite dealumination, since the local chemistry around $(AlO_2)^-$ sites in the ZSM-5 zeolites is not very different from that in Y-zeolites. The active Cu cations associated with $(AlO_2)^-$ sites are forced to change coordination and can move inside zeolite cages and channels as aluminum ions dislocate from the crystal framework, thus losing their tetrahedral coordination. This cation site loss causes permanent loss in catalytic activity, since $(AlO_2)^-$ cannot be restored again in the zeolite framework. STEM/EDX mapping (Figure 20) suggests that dealumination took place in the Cu(141)-ZSM-5 sample. The results of the hydrothermal stability tests are in good agreement with the STEM/EDX analysis.

Hydrated and hydrolyzed copper complexes may be formed when Cu-ZSM-5 is exposed to water vapor at reaction temperatures. These copper complexes are more mobile than Cu^{2+} cations alone, since the complexes have lower surface charge density. Therefore, hydrolyzed copper complexes migrate in zeolite cavities, which leads to the formation of Brönsted acids on the sites left behind. Upon dehydration, clusters form and aggregation leads to CuO particle formation and catalyst deactivation. A mechanism of Cu-ZSM-5 deactivation is proposed by the following simplified processes:

$$Cu^{2+} = Z \text{ (active isolated } Cu^{2+}) + 2\,H_2O \text{ <---> } Cu^{2+}(H_2O)_2\text{-}Z \qquad (1)$$

The electrostatic field of divalent Cu cations is assumed to generate protons through dissociation of water in the following way [32, 33]:

$$Cu^{2+}(H_2O)_2\text{-}Z \text{ <---> } [Cu(OH)(H_2O)]^+\text{-}Z\text{-}H^+ \qquad (2)$$

and,

$$[Cu(OH)(H_2O)]^+\text{-}Z\text{-}H^+ \text{ <---> } Cu(OH)_2 + H^+\text{-}Z\text{-}H^+. \qquad (3)$$

Finally, CuO is formed by the reaction:

$$Cu(OH)_2 \text{ <---> } CuO + H_2O \qquad (4)$$

Z is the ZSM-5 substrate, $Cu^{2+}(H_2O)_2$ and $[Cu(OH)]^+$ represent of hydrated and hydrolyzed Cu complexes, and H^+ is a Brönsted acid. In wet NO-decomposition, the steady state catalytic activities at different water vapor contents suggest that an equilibrium is established between Cu^{2+} and water vapor, otherwise 2% H_2O in the reaction stream is enough to deactivate all the active copper sites.

Upon water vapor removal from the reactant stream, only a part of the dry gas-catalytic activity is restored. This partial activity recovery must be mainly attributed to dehydration of the hydrolyzed or hydrated copper complexes. At the same time, CuO can be formed by reactions (3) and (4). Irreversible CuO particle formation causes permanent catalyst deactivation. It has been shown by XPS measurements that copper migrated out to surface regions can reversibly move back to zeolite. This is a strong indication that CuO particles were formed inside the zeolite channels. CuO particle formation would destroy the local crystal structure of the zeolite.

(9) Cerium effect on copper deactivation

Ce(60)-ZSM-5 electron micrographs show surface enrichment of cerium along with uniformly distributed Ce. As shown in Table 1, the Na/Al ratios are reduced confirming ion exchange, while the (3 Ce + Na)/Al ratio for the Ce(60)-ZSM-5 is greater than 1 indicating the formation of surface Ce. The above observations have been further confirmed by cerium photoluminescence [18] and XPS measurements.

The presence of Ce^{3+} cations in the Ce(60)/Cu(138)-ZSM-5 greatly improves the Cu-ZSM-5 wet-gas activity and has greater dry-gas activity recovery. Migration of more copper into zeolite surface regions and less CuO formation inside zeolite channels indicate that addition of cerium cations into Cu-ZSM-5 may change the energetics of copper hydration/migration so that CuO formation is not as favorable as in the Cu(141)-ZSM-5 catalyst. Ce^{3+} cations may also play the following roles: First, they physically or chemically block hydrated and hydrolyzed copper complex migration in the zeolite

channels. This suppresses copper aggregation, and also preserves more active sites because of the equilibrium in reactions (1) and (2). Second, cerium oxide in surface regions of the ZSM-5 crystal keeps the copper dispersed on the external surface, thus preventing it from sintering and makes it easier to migrate back, upon removal of water vapor. This would decrease CuO sintering. Another important role of ion-exchanged Ce in ZSM-5 is the stabilization of framework aluminum, thus preserving cation exchange sites. This is supported by the appearance of aluminum aggregates in the 500°C-20% H_2O catalytically used Cu(141)-ZSM-5 sample (Figure 22b), but not in the Ce(60)/Cu(138)-ZSM-5 catalyst (Figure 23c), as well as by the hydrothermal stability test results. The dual function of Ce cations in promoting Cu-ZSM-5 catalytic activity is also supported by the fact that Cu(60)/Cu(138)-ZSM-5 containing both ion-exchanged Ce and surface Ce showed higher wet-gas catalytic activity and higher activity recovery upon removal of water vapor for NO decomposition than either of the low-Ce exchanged Ce(11)/Cu(119)-ZSM-5 or the Ce-impregnated Cu-ZSM-5 materials.

Conclusion

"Excessively-exchanged" Cu-ZSM-5 is desirable as it is a more active catalyst for the NO decomposition reaction than under-exchanged Cu-ZSM-5. While a single-step ion-exchange from a dilute copper salt solution at pH > 6.5 can achieve a high copper loading in ZSM-5, not all the copper exists in the ion-exchanged state in the zeolite channels; a fraction of copper is on the surface, easily forming oxide particles after calcination. This surface deposited copper is inactive for NO decomposition. However, successive preparation from a cupric salt solution at pH = 5.7 will lead to active excessively exchanged Cu-ZSM-5 materials.

Alkaline earth and transition metal ion-exchanged ZSM-5 zeolites further exchanged with copper ions are active catalysts for the NO decomposition reaction in the presence or absence of oxygen and over a wide range of temperatures (350 - 600°C). For the same total copper exchange level, the Mg/Cu-Z catalysts show enhanced activity at high temperatures (450-600°C). Proper mode of ion exchange is crucial for a positive cocation effect. The NO decomposition rate is first order in partial pressure of NO over Cu(72)-ZSM-5, while it was first order at 400°C and 1.4 order at 600°C over

Mg(52)/Cu(66)-ZSM-5. Mg cations moderate the oxygen inhibition of the NO decomposition. The reaction order in O_2 was -0.5 over Cu(72)-ZSM-5, and -0.3 over Mg(52)/Cu(66)-ZSM-5.

Experimental results show that water vapor greatly decreases the NO decomposition activity of Cu-ZSM-5 catalysts due to the Cu^{2+} cation migration and CuO particle formation inside the zeolite crystal as indicated by the XRD, STEM/EDX and XPS analysis. The presence of both ion-exchanged Ce cations in the zeolite channels and Ce on the surface regions moderates the effect of water vapor on the Cu-ZSM-5 catalyst activity. The XRD and STEM/EDX results have identified less extensive CuO sintering for Ce(60)/Cu(138)-ZSM-5 than for Cu(141)-ZSM-5 in wet NO decomposition at 500°C. Therefore, the Ce cations are able to preserve a higher fraction of active sites in the catalysts even under severe steaming conditions.

Literature Cited

1. Iwamoto, M.; Furukawa, H.; Uemura, F.; Mikuriya, S.; Kagawa, S., *J. Chem. Soc. Chem. Commun.* **1986,** *15,* 1272- 73.
2. Iwamoto, M., in *Future Opportunities in Catalytic and Separation Technology,* Misono, M. et al ED.; Elserier: Amsterdam, **1990;** 121- 143.
3. Li, Y,; Hall, W. K., *J. Catal.* **1991,** 129, 202- 215.
4. Li, Y.; Armor, J., *Appl. Catal.* **1991,** *76,* L1.
5. Shelef, M., *Catal. Lett.* **1992,** *15,* 305- 310.
6. Iwamoto, M.; Yahiro, H.; Mine, Y.; Kagawa, S., *Chemm. Lett.* **1989,** 213.
7. Iwamoto, M.; Yahiro, H.; Torikai, Y.; Yoshioka, T.; Mizuno, N., *Chem. Lett.* **1990,** 1976.
8. Kagawa, S.; Ogawa, H.; Furukawa, H.; Teraoka, Y. *Chem. Lett.* **1991,** 407-410.
9. Zhang, Y.; Flytzani-Stephanopoulos, M. *Environmental Catalysis, ACS Symposium Series 552,* **1994,** pp. 7-21.
10. Iwamoto, M.; Yahiro, H.; Tanda, K.; Mizuno, N.; Mine, Y.; Kagawa, S. *J. Phys. Chem.* **1991,** *95,* 3727-30.
11. Li, Y.; Hall, W. K., *J. Phys. Chem.* **1990,** *94,* 6148.
12. Chu, P.; Dwyer, F. *Intrazeolite Chemistry, ACS Symposium Series 218,* **1983,** pp. 59-77.

13. Iwamoto, M.; Yahiro, H.; Torikai, Y.; Yoshioka, T.; Mizuno, N. *Chem. Lett.* **1990**, 1967.
14. Zhang, Y.; Leo, K.; Sarofim, A.; Flytzani-Stephanopoulos; Hu, Z. *Catal. Lett.* **1995** (in press).
15. Kucherov, A. V.; Slinkin, A. A.; Kondrat'ev, D.A.; Bondarenko, T. N.; Rubinshtein, A. M.; Minachev, Kh. M. *Kinet. and Catal.* **1985**, *26*, 353-358.
16. Kucherov, A. V.; Slinkin, A. A.; Goryashenko, S. S.; Slovetskaja, K. I. *J. Catal.* **1989**, *118*, 459-465.
17. Shelef, M. *Catal. Lett.* **1992**, *15*, 305-310.
18. Zhang, Y, *Ph.D. Thesis*, Massachusetts Institute of Technology, Cambridge,*(work in progress).*
19. Li, Y.; Armor, J. *Appl. Catal.* **1991**, *76*, L1-8.
20. Flytzani-Stephanopoulos, M., Sarofim, A. F., Zhang, Y., Quarterly Technical Progress Report No. 7 to DOE, April- June 1993, Grant No. DE-FG22-91PC91923.
21. Zhang, Y.; Sun, T., Sarofim, A. F.; and Flytzani-Stephanopoulos, M., ACS Symposium on NOx Reduction, Preprints, 39, 171, (1994); also in *NOx Reduction*, ed. by G. Marcelin, ACS, Washington, DC (in press).
22. Grinsted, R.A.; Jen, H.W.; Montreuil, C.N.; Rokosz, M.J.; Shelef, M., *Zeolites*, **1993**, *13*, 602.
23. Kharas, K.C.C.; Robota, H.J.; Datye, A., *ACS Symposium Series 552*, edited by Armor, J., 39, (1994).
24. Shpiro, E. S.; Grüner, W.; Joyner, R. W.; and Baeva, G. N., *Catal. Lett.*, **1994**, *24*, 159.
25. Haack, L. P.; and Shelef, M., *ACS Symposium Series 552*, edited by Armor, J., 66-67, (1994).
26. Suib, S. L.; Stucky, G. D.; and Blattner, R. J., *J. Catal.*, **1980**, *65*, 179.
27. Suzuki, K.; Sano, T.; Shoji, H.; Murakami, T.; Ikai, S.; Shin, S.; Hagiwara, H.; Takaya, H., *Chem Lett.* **1987**, 1507-1510.
28. Fujisawa, K.; Sano, T.; Suzuki, K.; Okado, H.; Kawamura, K.; Kohtoku, Y.; Shin, S.; Hagiwara, H.; Takaya, H., *Chemi. Soc. Japan*, **1987**, *60*, 791-793.
29. Kerr, G.T., *J. Catal.* **1969**, *15*, 200.
30. Kerr, G.T., *J. Phy. Chem.* **1968**, *72*, 2549.
31. McNicol, B.D.; Pott, G.T., *J. Catal.* **1972**, *25*, 223.
32. Uytterhoeven, J.B.; Schohheydt, R.; Liengme, B.V.; Hall, W.K., *J. Catal.* **1969**, *13*, 425.

33. Jacobs, P.A., in "Carboniogenic Activity of Zeolites," p.45, Elsevier, Amsterdam, 1977.

Table 1. Cu-ZSM-5 Catalyst Preparation at Various pH[1]

Catalyst	Si/Al[2]	Cu/Al[2]	Na/Al[2]
as-received Na-ZSM-5	21.5 (supplier's)		1.0
First set of samples[3]			
Cu(40)-ZSM-5(4.5)	19.1	0.20	0.09
Cu(74)-ZSM-5(4.9)	19.2	0.37	0.20
Cu(102)-ZSM-5(5.7)	19.0	0.51	0.20
Cu(97)-ZSM-5(6.0)	19.0	0.48	0.18
Cu(154)-ZSM-5(6.5)	18.6	0.77	0.11
Cu(165)-ZSM-5(7.0)	19.0	0.83	0.11
Cu(154)-ZSM-5(7.5)	18.4	0.77	-
Cu(136)-ZSM-5(5.7/7.0)[4]	18.1	0.68	-
Second set of samples[5]			
Cu(10)-ZSM-5(5.7)	20.5	0.05	0.80
Cu(30)-ZSM-5(5.7)	19.1	0.15	0.49
Cu(50)-ZSM-5(5.7)	19.4	0.25	0.37
Cu(73)-ZSM-5(5.7)	21.3	0.37	0.20
Cu(97)-ZSM-5(5.7)	21.9	0.48	0.13
Cu(102)-ZSM-5(5.7)	19.0	0.51	0.20
Cu(142)-ZSM-5(5.74)[6]	20.3	0.71	0.00

1 pH measured before contacting Na-ZSM-5 with the aqueous cupric acetate solution.

2 Si, Al, Cu and Na contents as measured by ICP.

3 Cu ion-exchanged with Na-ZSM-5 at room temperature for 19 hours once.[4] Cu first ion-exchanged with Na-ZSM-5 at room temperature and pH= 5.8 for 19 hours, then gradually adding aqueous ammonia into the slurry of Na-ZSM-5 and cupric acetate solution to pH=7.0.

5 Cu ion-exchanged with Na-ZSM-5 at room temperature for 19 hours once.

6 Cu ion-exchanged with Na-ZSM-5 at room temperature for 19 hours thrice.

Table 2. Summary of Catalyst Syntheses and Properties

Catalysts	Si/Al	Cu/Al[2]	Cocation/Al[2]	Na/Al[2]	Cu exchange
Parent zeolite [1]	21.5			1.0	
Cu-Z	20.3	0.705 (141%)	-	~0	thrice, RT
Cu-Z	19.9	0.36 (72%)	-	0.25 (25%)	once, RT
Mg/Cu-Z[3]	18.0	0.456 (91%)	0.202 (40%)	~0	twice, RT
Mg/Cu-Z[4,5]	17.1	0.430 (86%)	0.170 (34%)	~0	twice, RT
Mg/Cu-Z[3,5]	19.5	0.33 (66%)	0.26 (52%)	~0	twice, RT
Ba/Cu-Z[3,5]	22.1	0.63 (126%)	0.025 (5%)	~0	twice, RT
Y/Cu-Z[3,5]	22.4	0.675 (135%)	0.045 (13%)	~0	twice, RT
Ce/Cu-Z[3,5]	19.5	0.596 (119%)	0.036 (11%)	~0	twice, RT
Ce/Cu-Z[3,5]	19.8	0.69 (138%)	0.20 (60%)	~0	thrice, RT
Ce-Z	20.4		0.034 (11%)	0.72	once
Ce-Z	20.7		0.088 (26%)	0.58	thrice
Ce-Z	20.8		0.20 (60%)	0.52	thrice

1. ZSM-5: SMR-2670-1191, as received from Davison Div.,W.R. Grace. Co.
2. The values in parentheses are ion exchange levels, on the basis of Al content as measured by ICP.
3. Cocations exchanged once with Na/ZSM-5 at 85°C for 2 hours.
4. Cocation exchanged once with Na/ZSM-5 overnight at RT.

5. The cocation-exchanged ZSM-5 catalysts were dried in air at 100°C overnight, and calcined at 500°C for 2 hours.

Table 3. Effects of Cations on Hydrothermal Stability

The following samples were washed with 0.05M HNO3 for 4 hours, then with 0.01M NaNO3 for 10 hours after steaming. The samples were then dried at 100°C for 10 hours and calcined at 500°C for 2 hours.

Catalysts (cation-ZSM-5)	Si/Al	Cu/Al (remaining Cu)	Cu/Al (removed Cu)
Cu(141)-1	20.3	0.17	0.54
Cu(141)-2	22.8	0.30	0.41
Cu(141)-3	20.2	0.13	0.58
Cu(141)-4	21.1	0.07	0.64
Ce(40)/Cu(135)-1	21.5	0.19	0.49
Ce(40)/Cu(135)-2	22.8	0.32	0.36
Ce(60)-2,5	22.0	-	-

The following are ICP measurements after the above samples were ion-exchanged with 0.007 M $Cu(ac)_2$ at room temperature for 20 hours thrice.

Catalysts	Si/Al	Cu/Al	Cu/Al(re-exchanged)
Cu(141)-1	20.4	0.65	0.47
Cu(141)-2	22.9	0.57	0.27
Cu(141)-3	20.3	0.68	0.56
Cu(141)-4	21.3	0.78	0.71
Ce(40)/Cu(135)-1	21.0	0.77	0.60
Ce(40)/Cu(135)-2	22.9	0.67	0.35
Ce(60)-2,5	22.1	-	0.41
Na-ZSM-56	22.1		0.10

---

1. at 500°C; catalytically steamed in 20% H2O- 2% NO- He for 10 hours and dried in 2% NO+ He for 20 hours;
2. at 600°C; catalytically steamed in 20% H2O- 2% NO- He for 10 hours

and dried in 2% NO - He for 20 hours;

3. at 500°C steamed in 20% H2O- 4% O2- He for 10 hours and dried in 2% NO-He for 20 hours;
4. reacted in 2% NO+ He for 20 hours at 500°C;
5. steamed and dried at 600°C;
6. at 600°C steamed in 20% H2O- 2%O2- He for 10 hours and dried in 2% NO - He for 20 hours.

Table 4. Micropore Volume of Catalysts[1]

catalysts	fresh	catalytically used[2]	volume loss
Cu(141)-ZSM-5	0.178 cm3/g	0.145 cm3/g at 500°C	18.6%
Ce(60)/Cu(138)-ZSM-5	0.159 cm3/g	0.136 cm3/g at 500°C	14.6%
		0.109 cm3/g at 600°C	31.7%
Na-ZSM-5	0.147 cm3/g	0.109 cm3/g at 500°C	26.0%
		0.0 cm3/g at 600°C	100%

1. Measured by n-hexane adsorption.
2. In 20% H2O - 2% NO - He for 10 hours, then in 2% NO -He for 20 hours.

Table 5 Activity Comparisons of Copper Re-exchanged ZSM-5 with Steamed and Fresh Cu-ZSM-5

Catalysts	NO Conversion to N_2 (%)[a]	Corresponding Active Cu (%)[b]
Cu re-exchanged Cu(94)-ZSM-5 from 500°C-steamed Cu(141)-ZSM-5	28.0	42
Cu re-exchanged Cu(120)-ZSM-5 from 500°C-steamed Ce(40)/Cu(135)-ZSM-5	30.1	43
Cu exchanged Cu(108)-ZSM-5 from 600°C-steamed Ce(60)-ZSM-3	13.7	31
Cu(141)-ZSM-5 after 500°C-steaming	29.0	42.5
Ce(40)-ZSM-5 after 500°C-steaming	53.0	61
Fresh Cu(94)-ZSM-5	72	94
Fresh Cu(108)-ZSM-5	77.5	108
Fresh Cu(120)-ZSM-5	82.5	120

a in 2% NO- He at 500°C and W/F = 1.0 g s/cm^3

b Active copper exchange level was estimated based on catalytic activity from Figure 2.

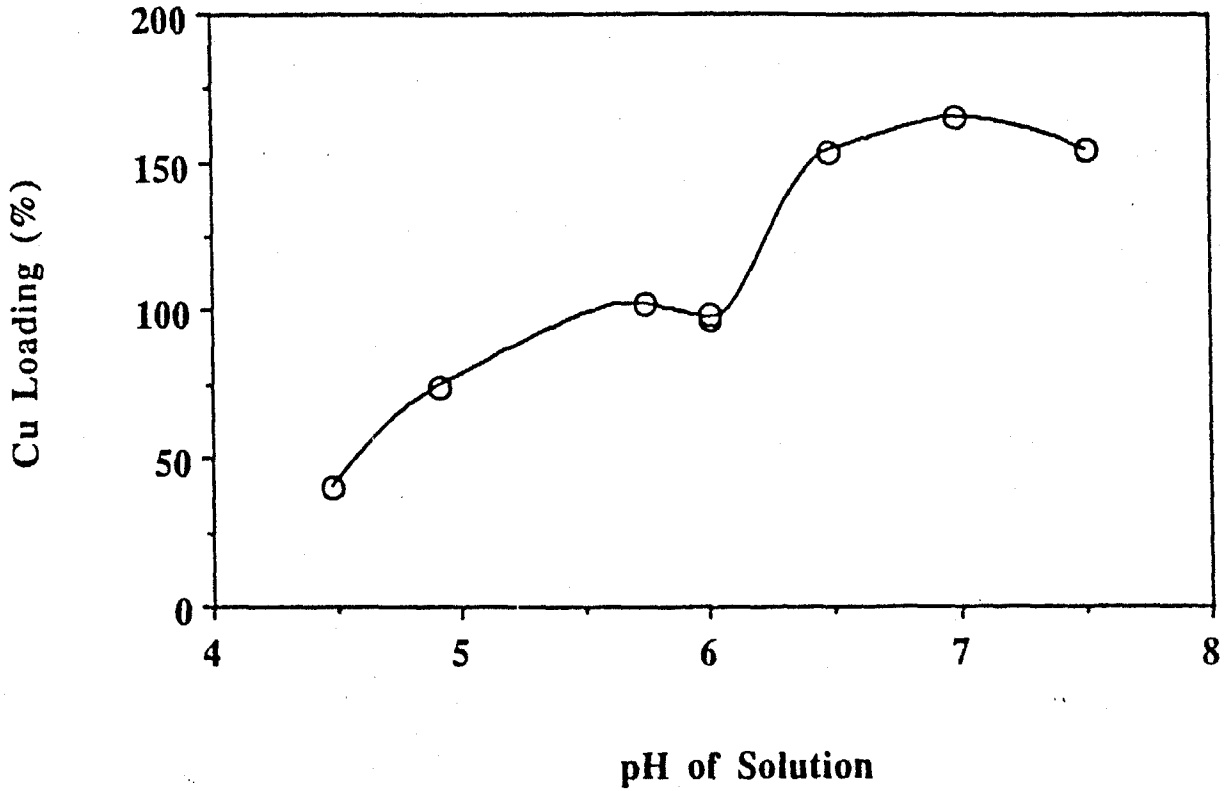

Figure 1a. Dependence of Cu loading on pH of cupric acetate solution: $Cu(ac)_2$ concentration: 0.007 M, RT, exchange time: 19 h.

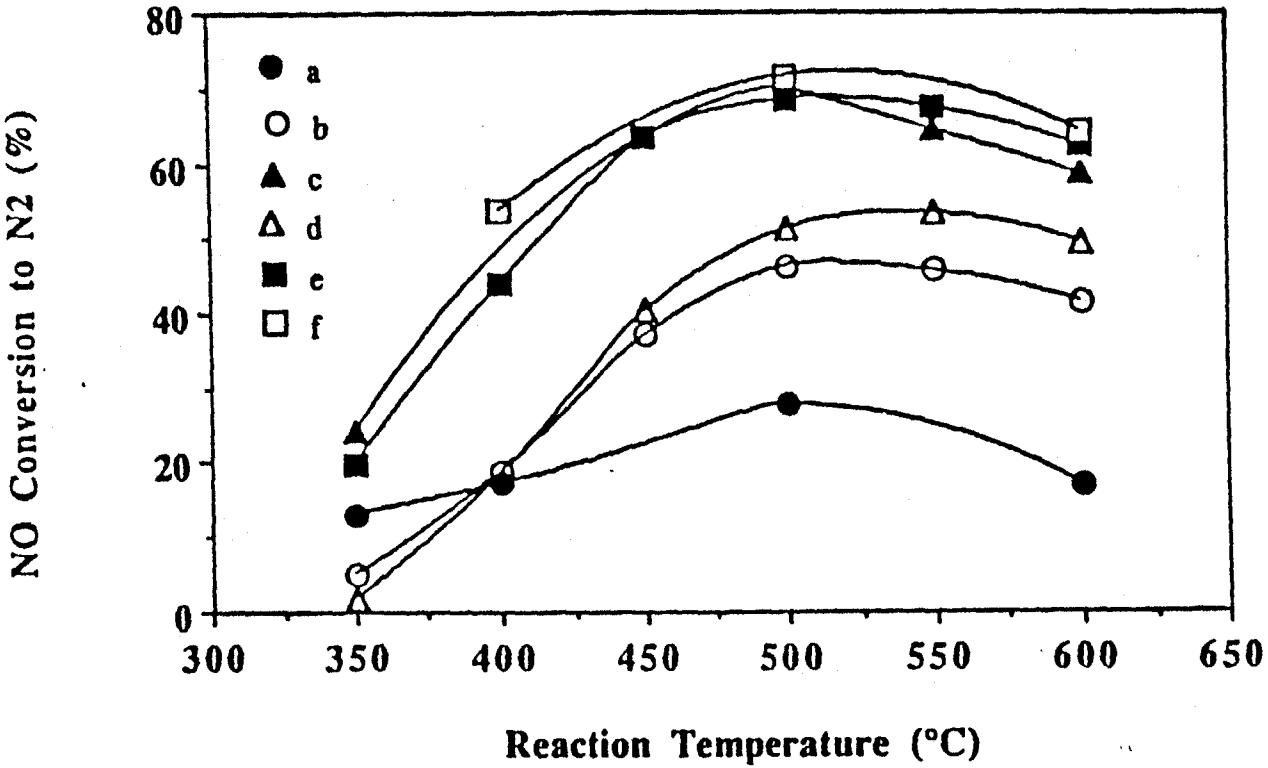

Figure 1b. Effects of catalyst preparation on catalytic activity for NO conversion to N2 in 2%NO+ He and 1g s/cc (STP): (a) Cu(40)-ZSM-5(4.5); (b) Cu(74)-ZSM-5(4.9); (c) Cu(102)-ZSM-5(5.7); (d) Cu(97)-ZSM-5(97); (e) Cu(165)-ZSM-5(7.0); (f) Cu(154)-ZSM-5(7.5).

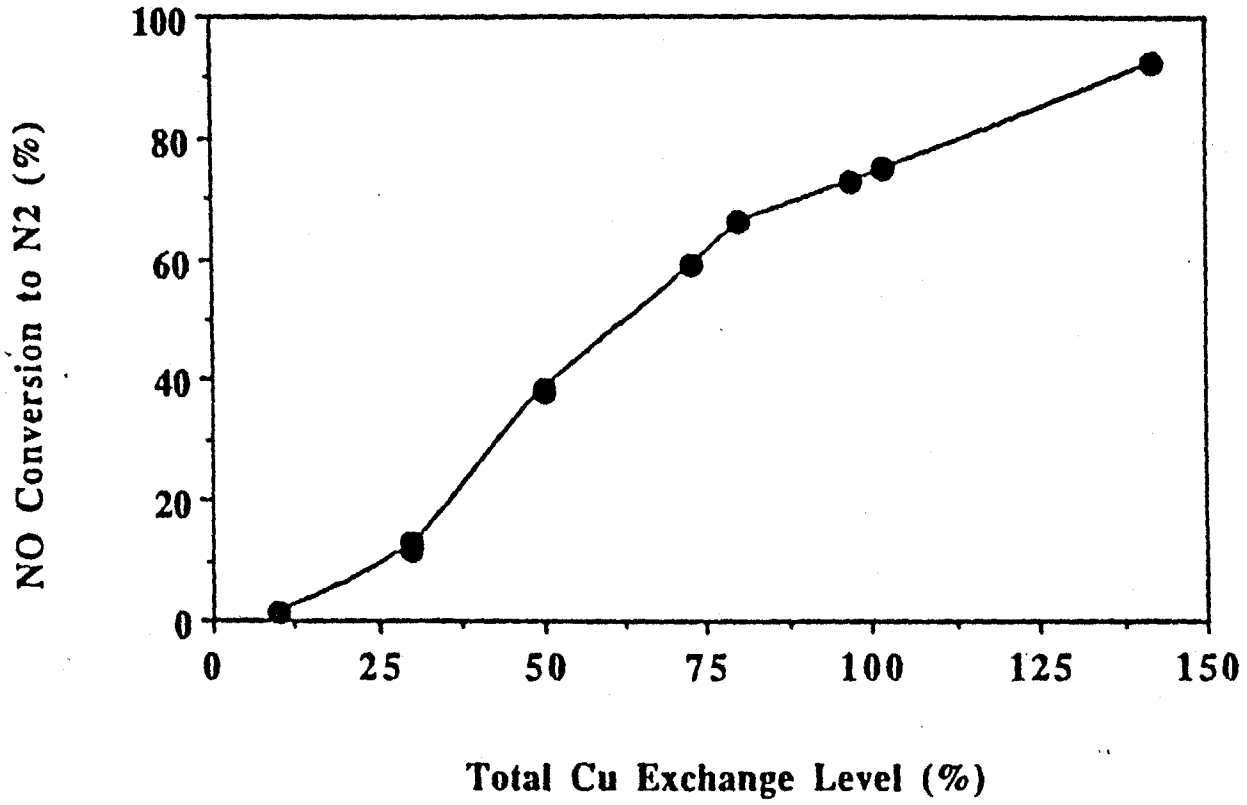

Figure 2. The effect of Cu exchange level on the catalytic activity or NO decomposition in 2%NO+ He, W/F = 1g s/cc (NTP) and 500°C.

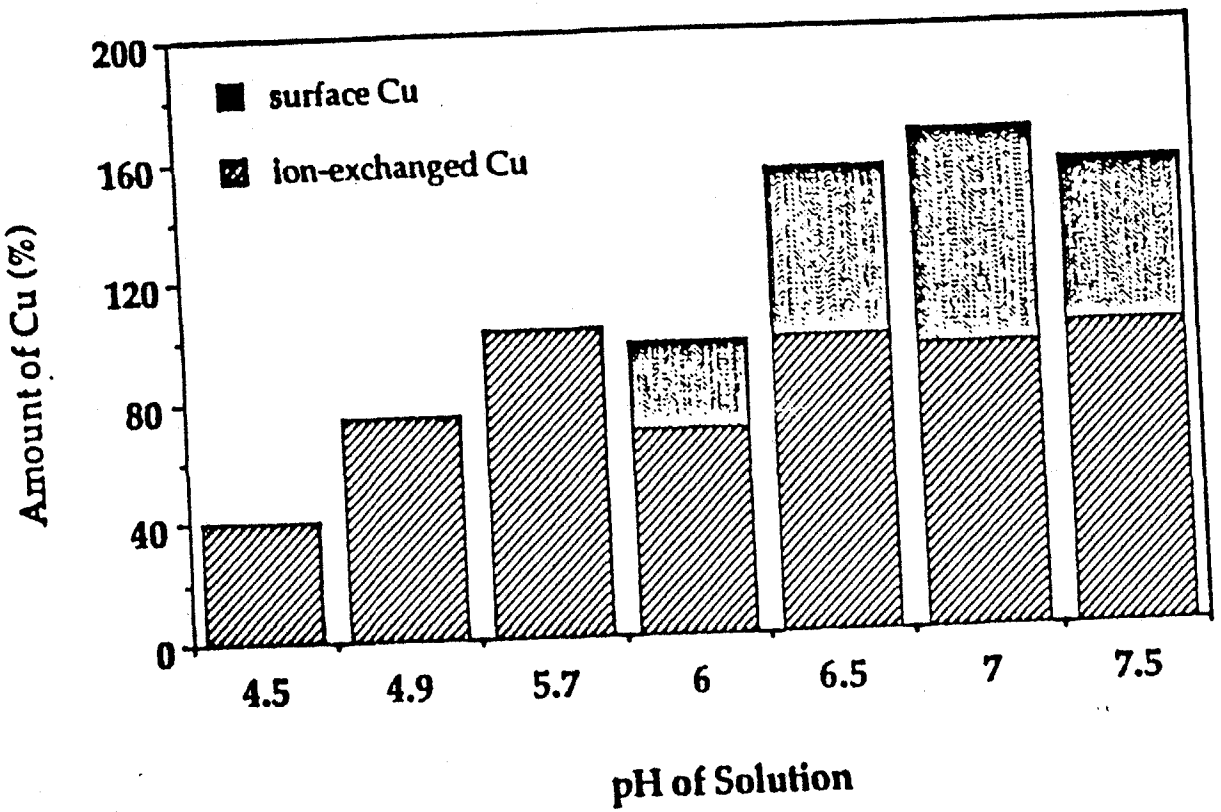

Figure 3. Cu distribution in the first set of catalysts.

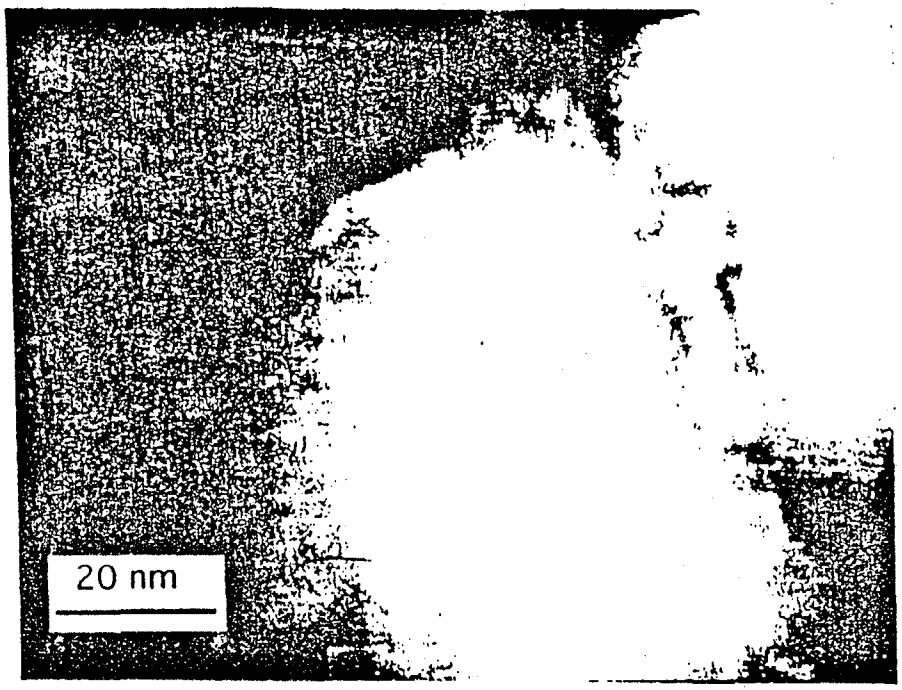

Figure 4. STEM dark field micrograph of the calcined Cu(165)-ZSM-5(7.0) showing copper aggregates (bright spots).

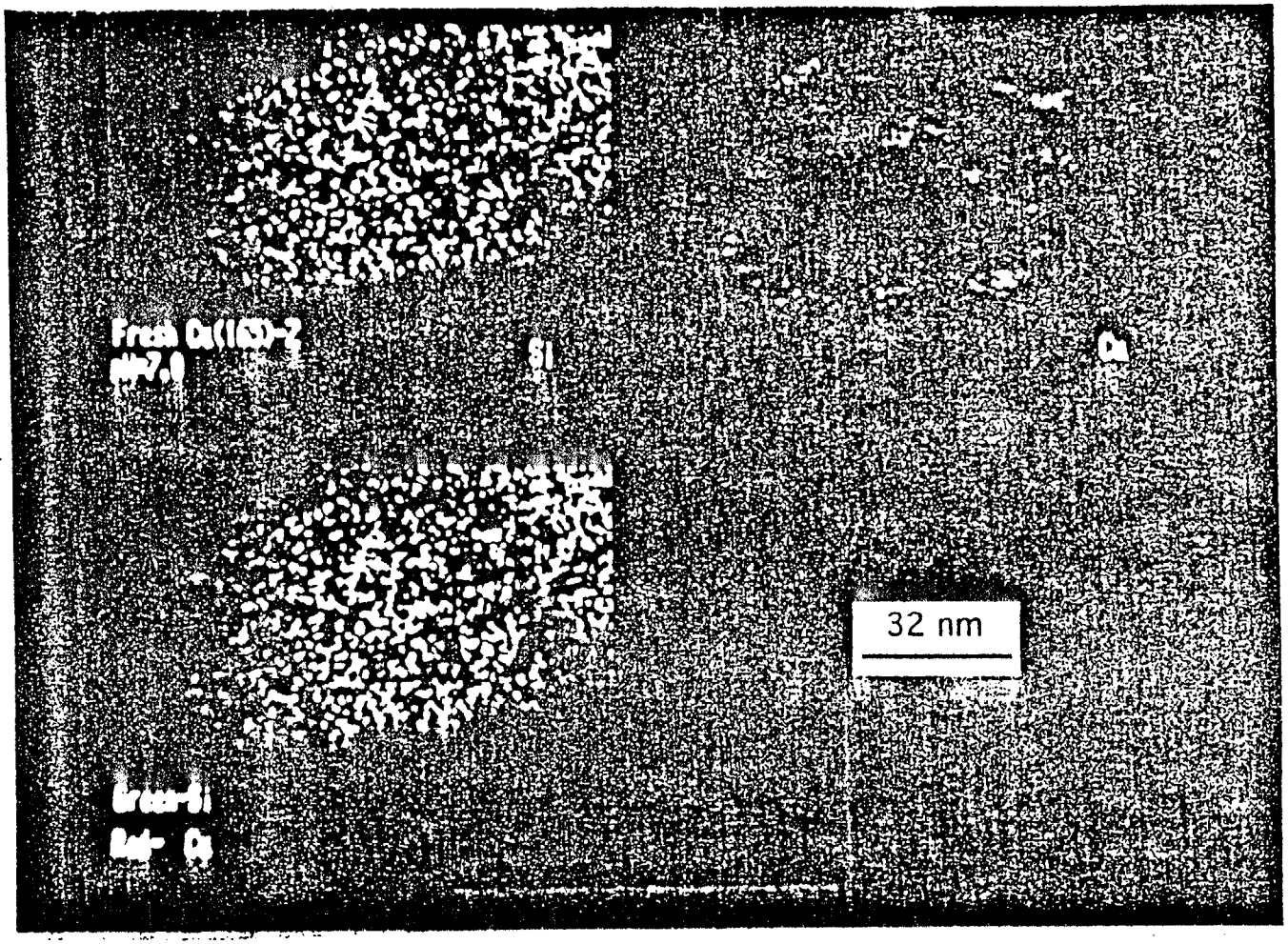

Figure 5. X-ray mapping of Si and Cu in the calcined Cu(165)- ZSM-5(7.0) sample.

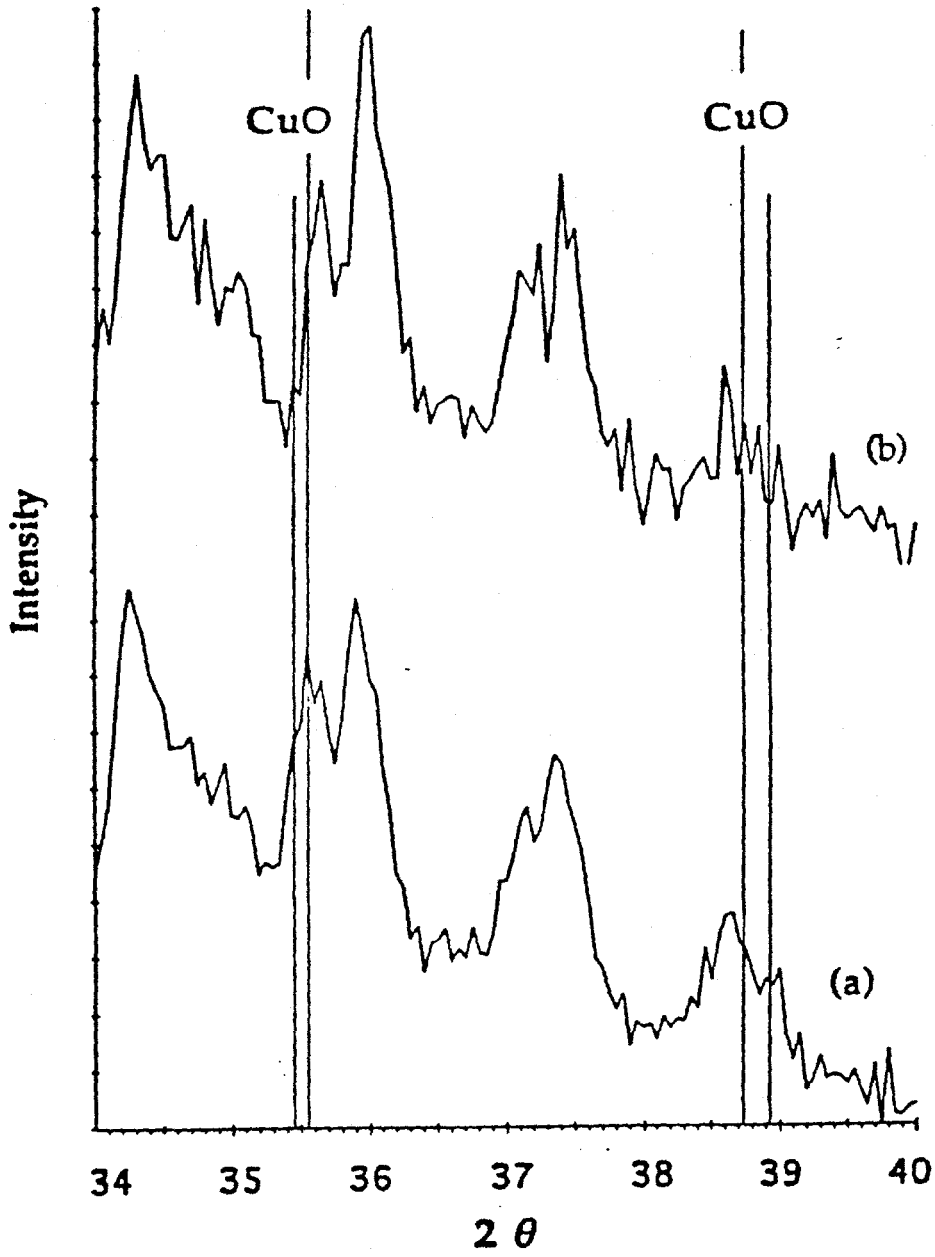

Figure 6. XRD patterns of (a) 500°C, 2h-calcined Cu(154)-ZSM-5(7.5) showing CuO formation, and (b) parent Na-ZSM-5.

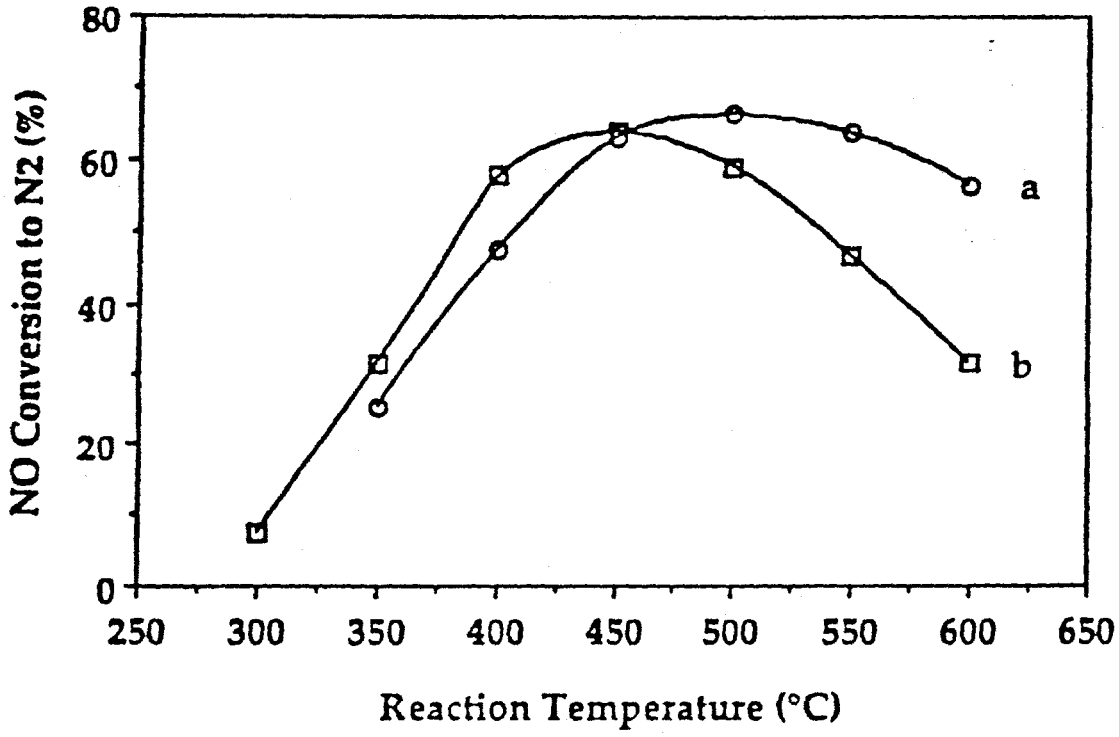

Figure 7. Comparison of NO conversion to N2 over (a)Mg(52)/Cu(66)-ZSM-5; (b) Cu(72)-ZSM-5 at 2%NO and W/F= 1 g s/cc (NTP).

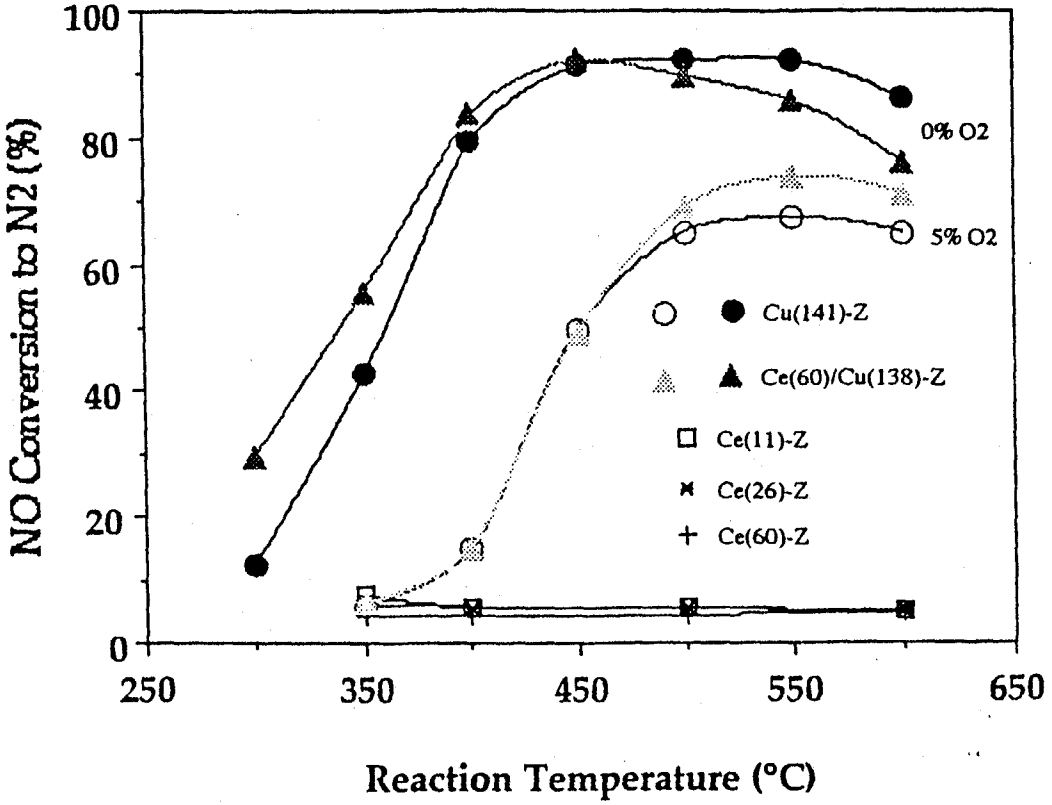

Figure 8. NO conversion over Ce-ZSM-5, Cu-ZSM-5 and Ce modified Cu-ZSM-5 catalysts in 2% NO - 0% (or 5%) O2 - He, at W/F = 1.0 g s/cc (NTP).

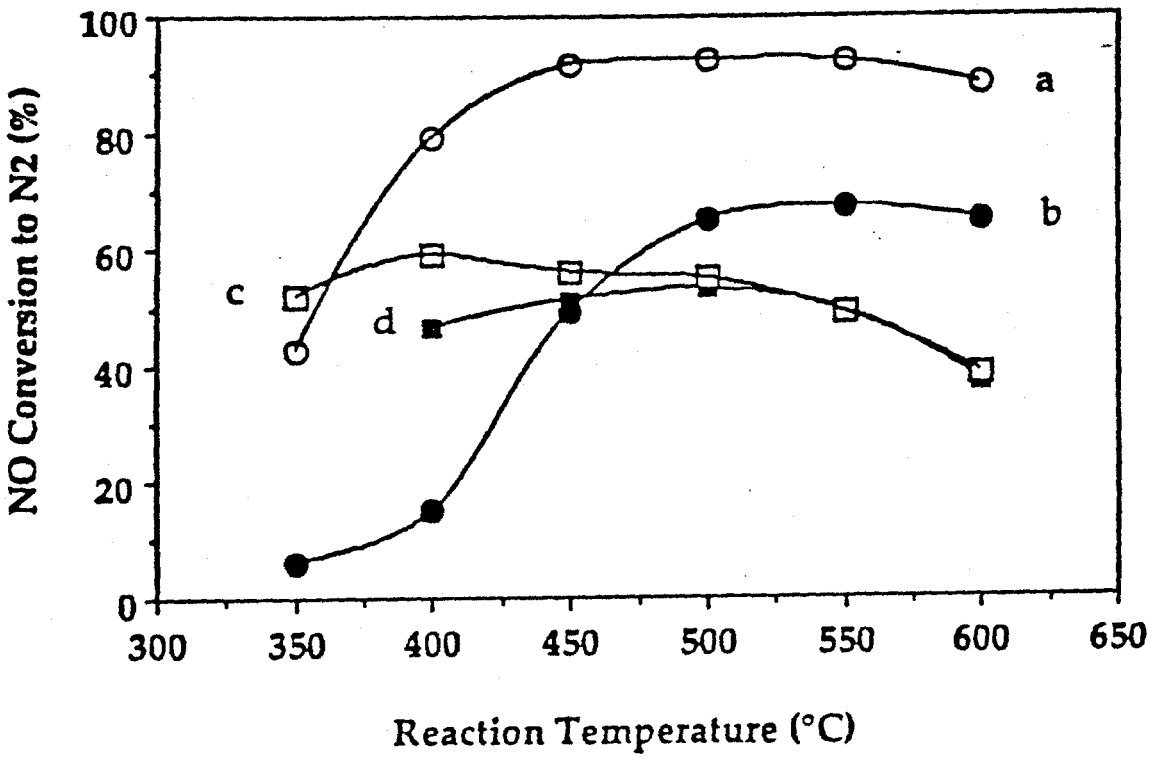

Figure 9. Effect of O2 and NO concentrations on the Cu(141)-ZSM-5 activity for NO decomposition at W/F = 1 g s/cc (NTP); (a) 2% NO - 5% O2 - He; (b) 2% NO - 5% O2 -He; (c) 0.2% NO - 0% O2 - He; (d) 0.2% NO - 5% O2 -He.

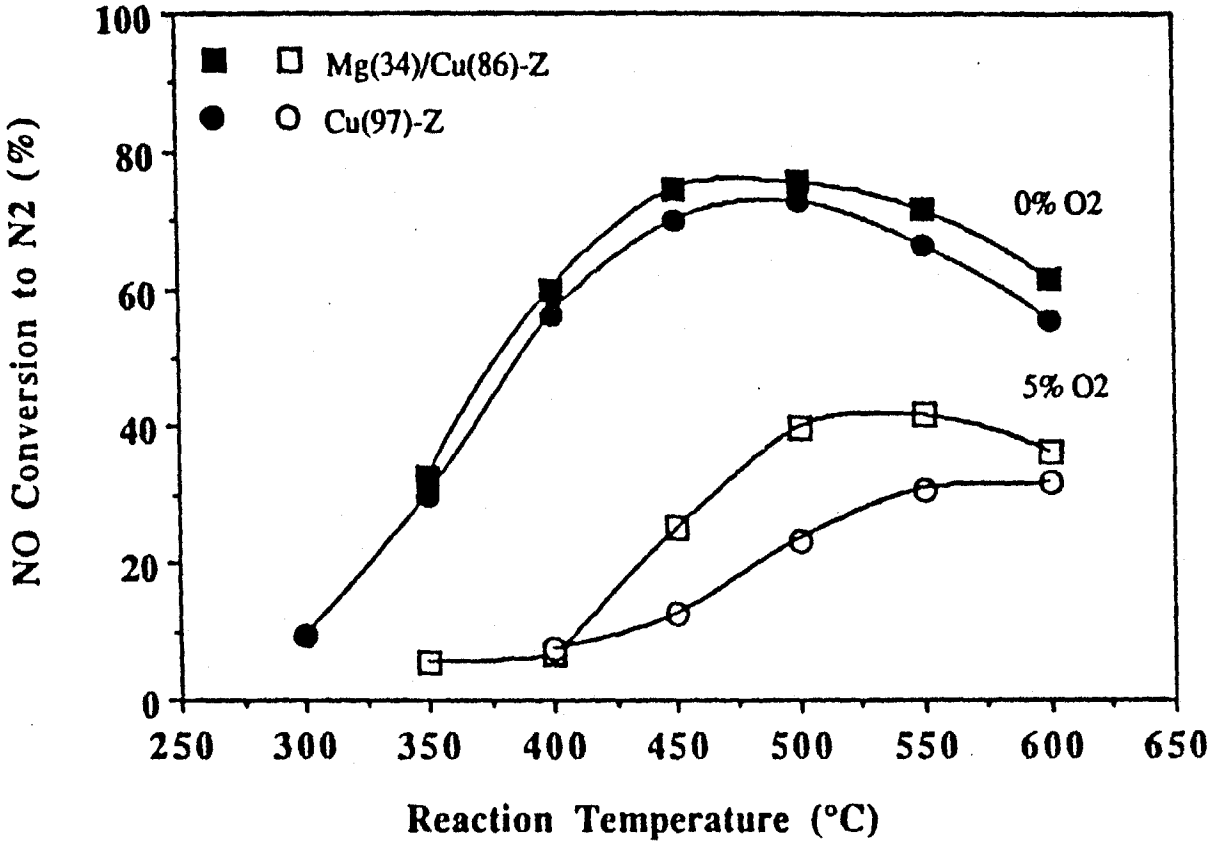

Figure 10. Activity comparison of Cu(97)-ZSM-5 with Mg(34)/Cu(86)-ZSM-5 in 2% NO - He at W/F = 1 g s/cc (NTP); 0 and 5% O2.

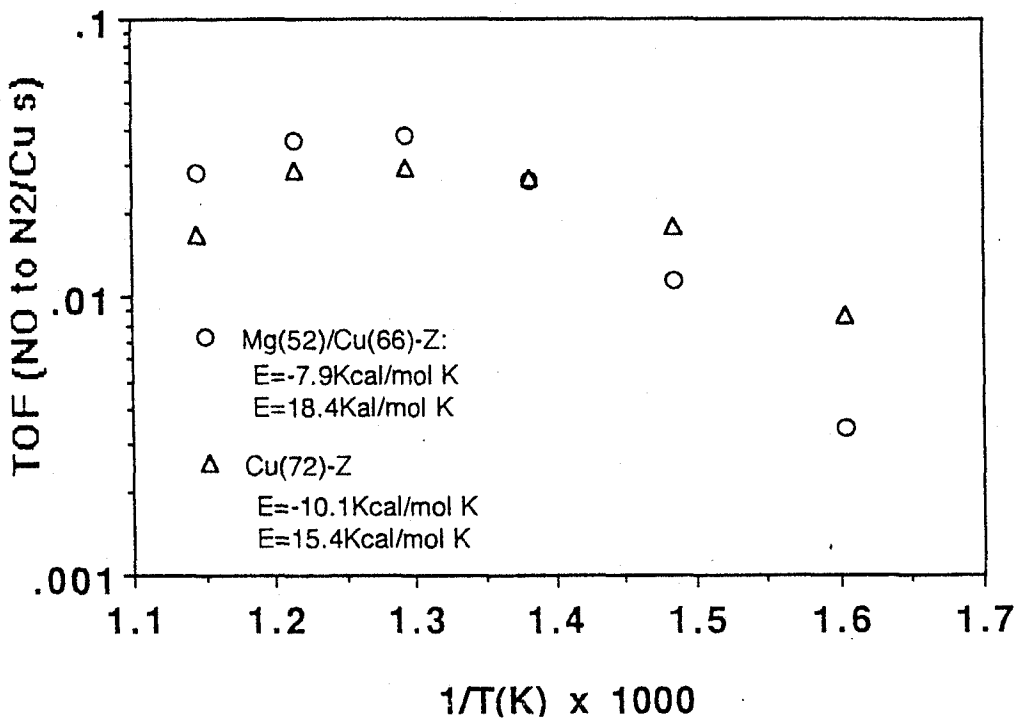

Figure 11. Arrhenius-type plots of the turnover frequencies of Cu(72)-ZSM-5 and Mg(52)/Cu(66)-ZSM-6 in 4% NO- He at W/F= 0.03 g s/cc (NTP).

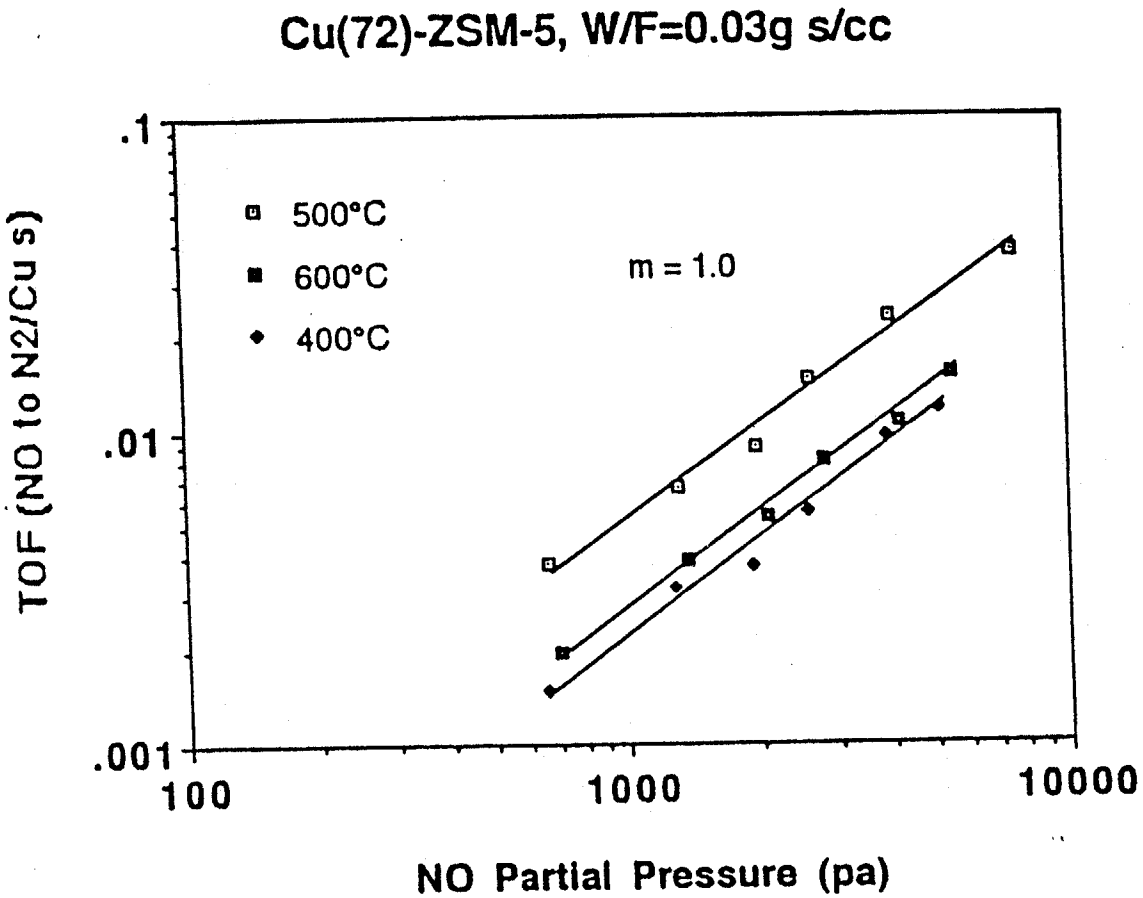

Figure 12a. NO decomposition rate dependence on the partial pressure of NO over Cu(72)-ZSM-5 at W/F = 0.03 g s/cc (NTP).

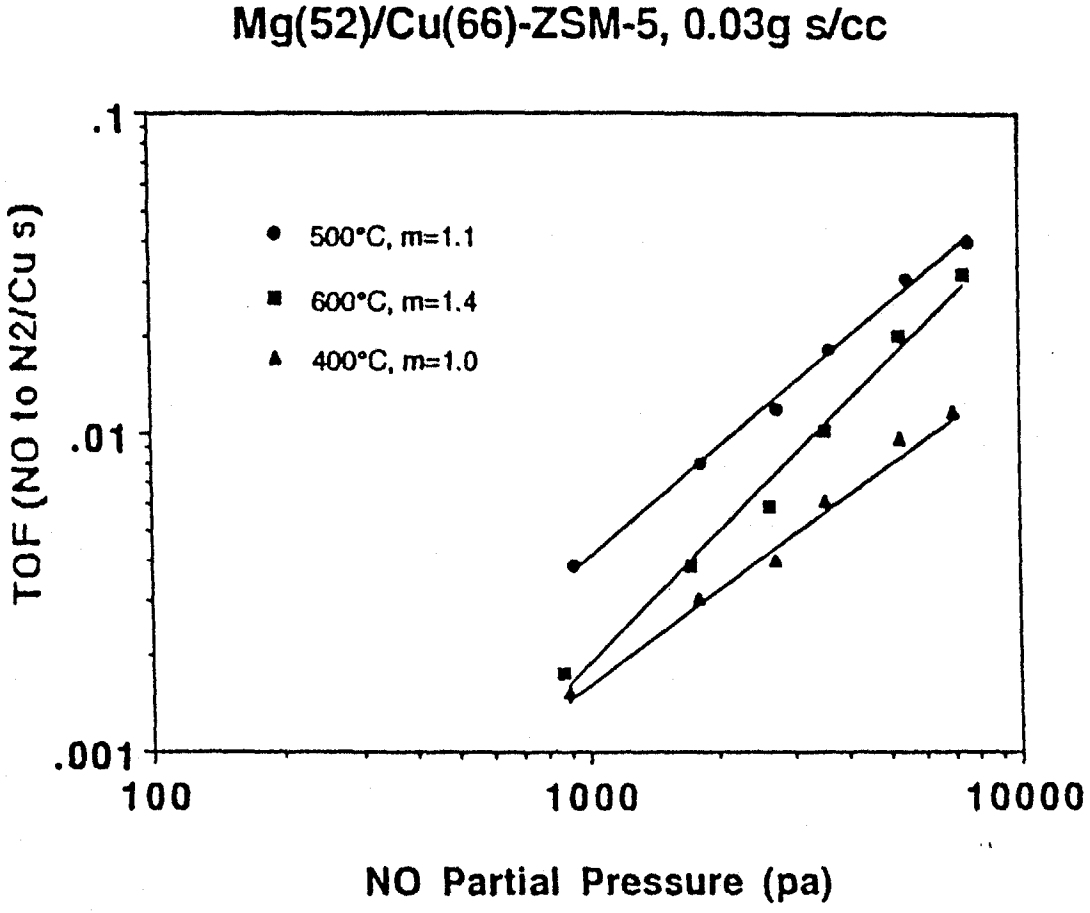

Figure 12b. NO decomposition rate dependence on the partial pressure of NO over Mg(52)/Cu(66)-ZSM-5 at W/F = 0.03 g s/cc (NTP).

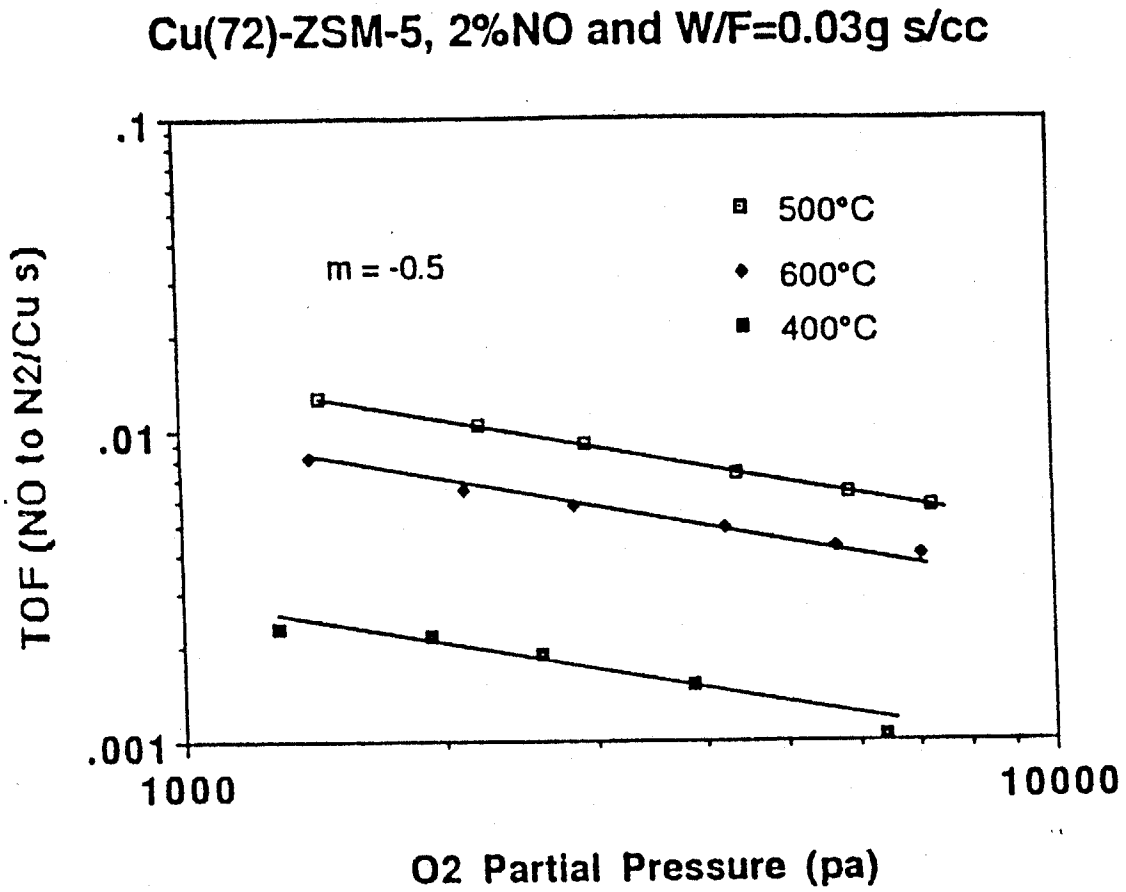

Figure 13. NO decomposition rate dependence on the partial pressure of O2 over Cu(72)-ZSM-5 in 2% NO - He at W/F = 0.03 g s/cc (NTP).

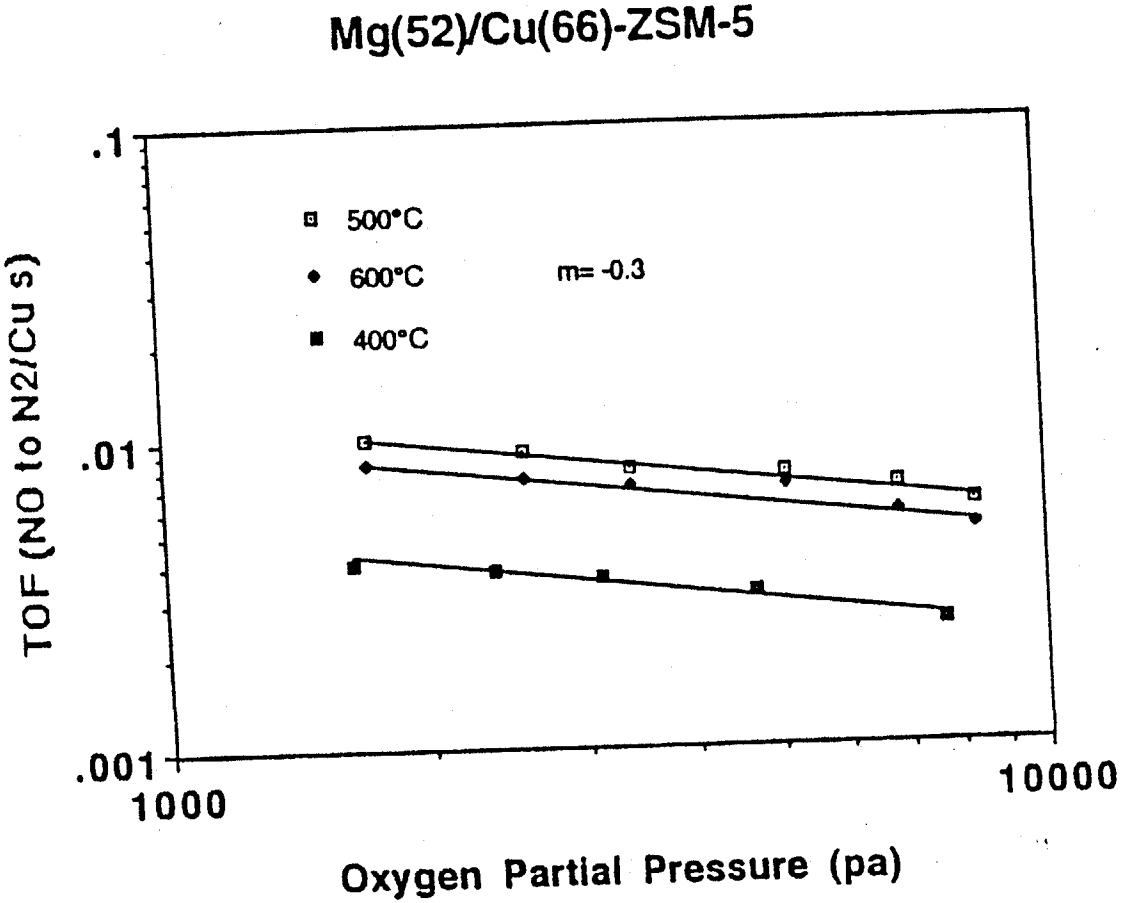

Figure 14. NO decomposition rate dependence on the partial pressure of O2 over Mg(52)/Cu(66)-ZSM-5 in 2% NO - He at W/F = 0.03 g s/cc (NTP).

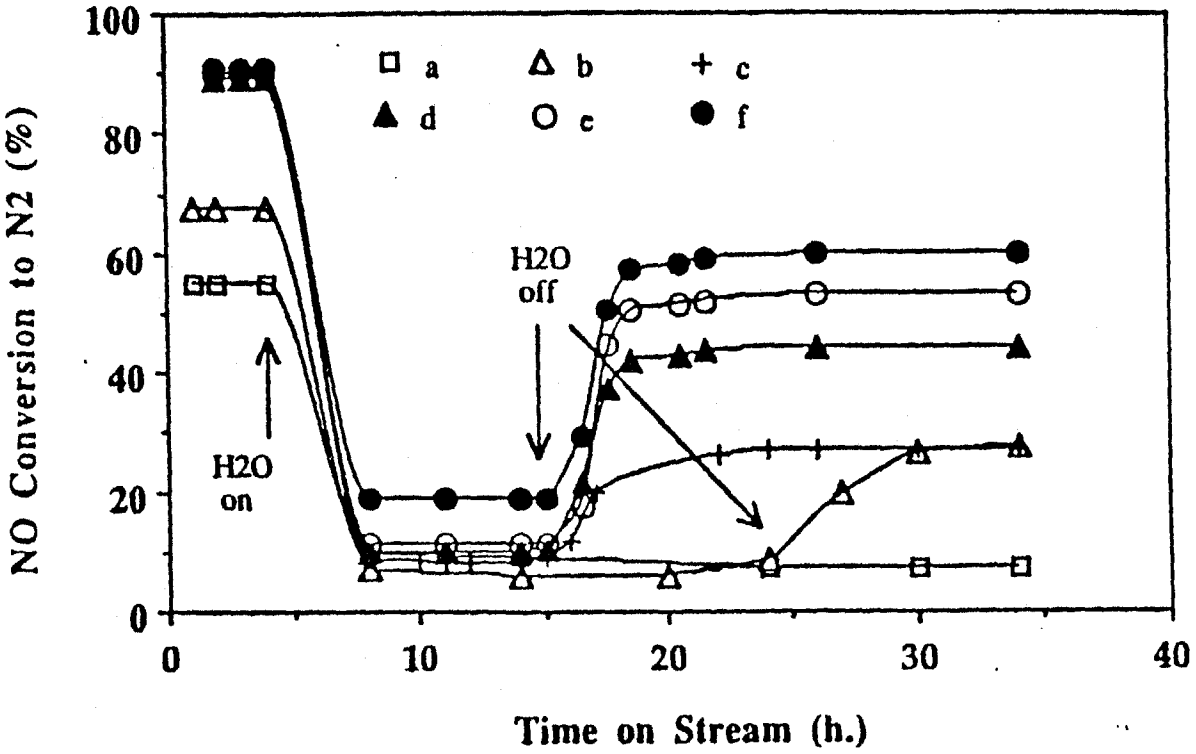

Figure 15. Effect of H2O vapor on the NO conversion to N2 over (a) Cu(72)-ZSM-5; (b) Mg(52)/Cu(66)-ZSM-5; (c) Cu(141)-ZSM-5; (d) Ba(5)/Cu(126)-ZSM-5; (e) Y(13)/Cu(135)-ZSM-5; (f) Ce(60)/Cu(138)-ZSM-5 catalysts in 20% H2O - 2% NO - He at 500°C, W/F = 1 g s/cc (NTP).

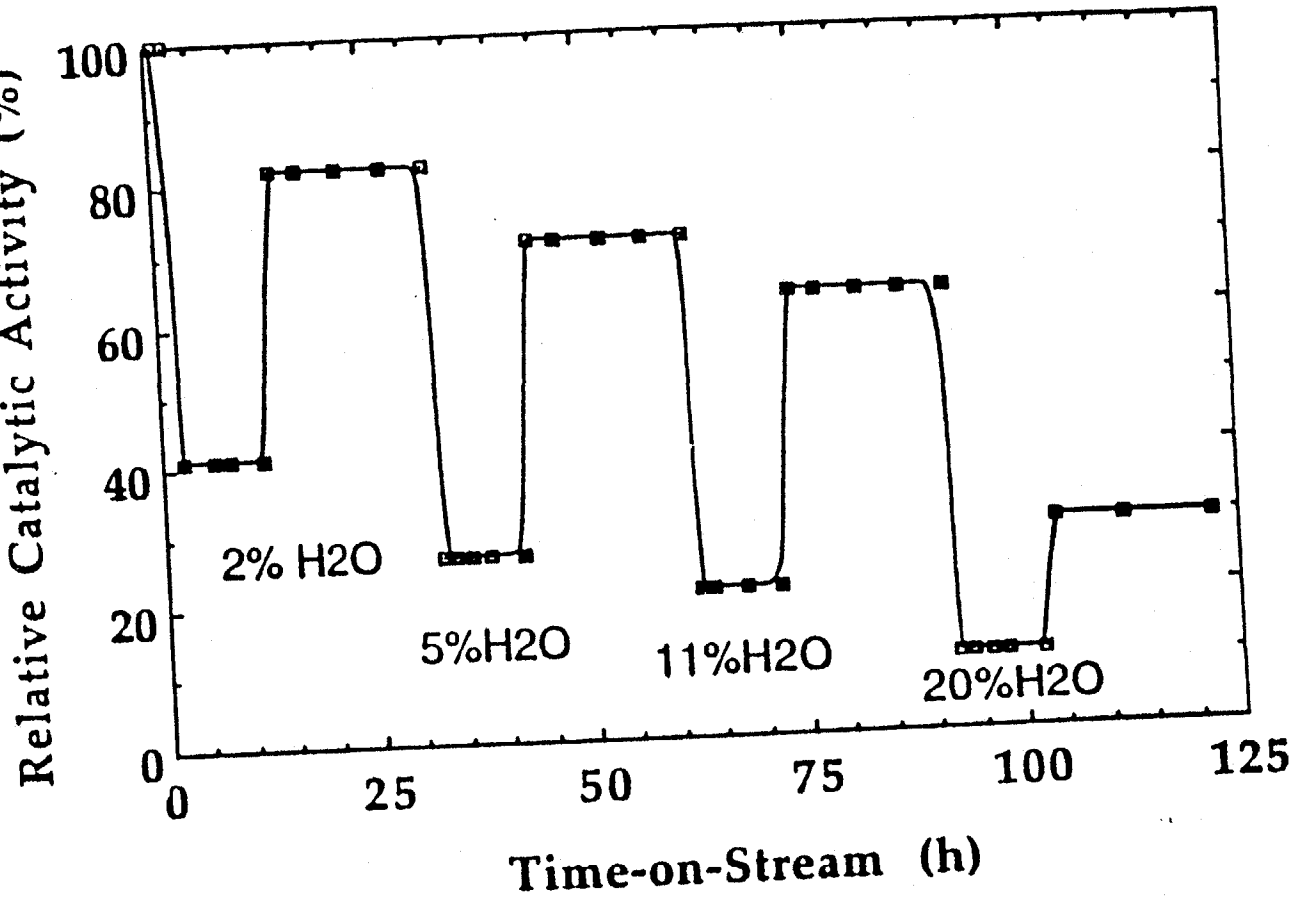

Figure 16. Cyclic performance of Cu(141)-ZSM-5 in dry/wet NO decomposition in 2% NO - He, at W/F = 1 g s/cc (NTP) and 500°C.

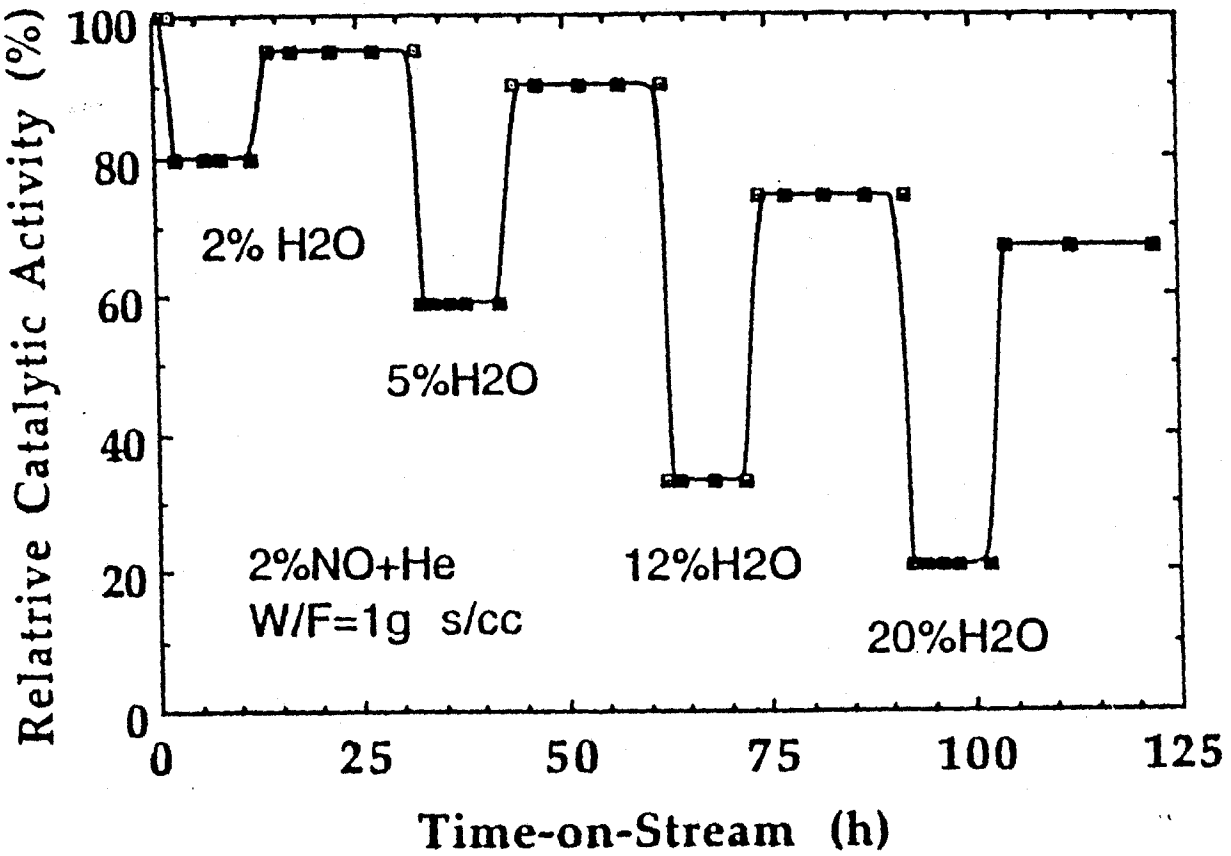

Figure 17. Cyclic performance of Ce(60)/Cu(138)-ZSM-5 in dry/wet NO decomposition in 2% NO - He, at W/F = 1 g s/cc (NTP) and 500°C.

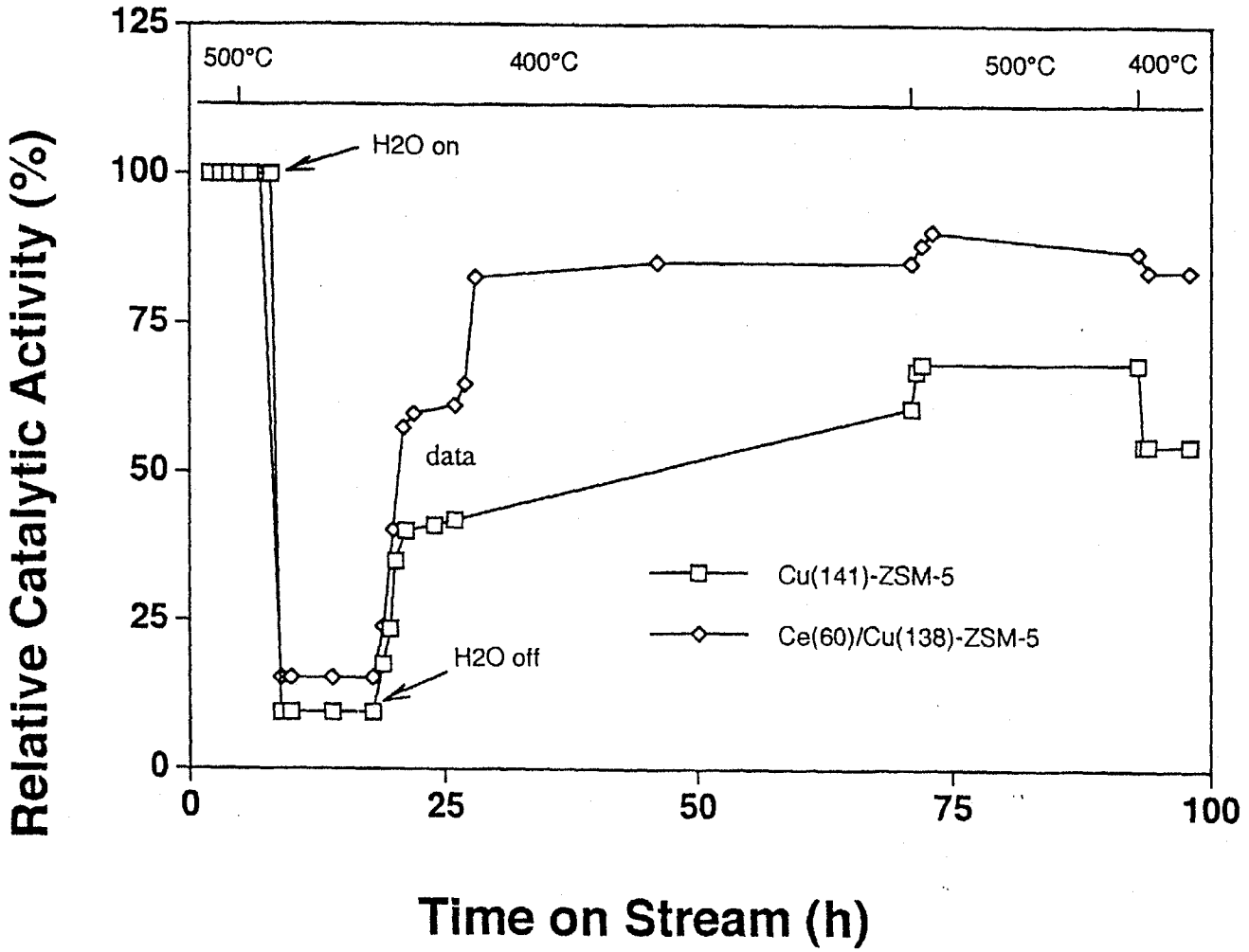

Figure 18. Effect of H2O vapor on the NO conversion to N2 over Cu(141)-ZSM-5 and Ce(60)/Cu(138)-ZSM-5 catalysts in 20% H2O - 2% NO - He at 400°C, W/F = 1 g s/cc (NTP).

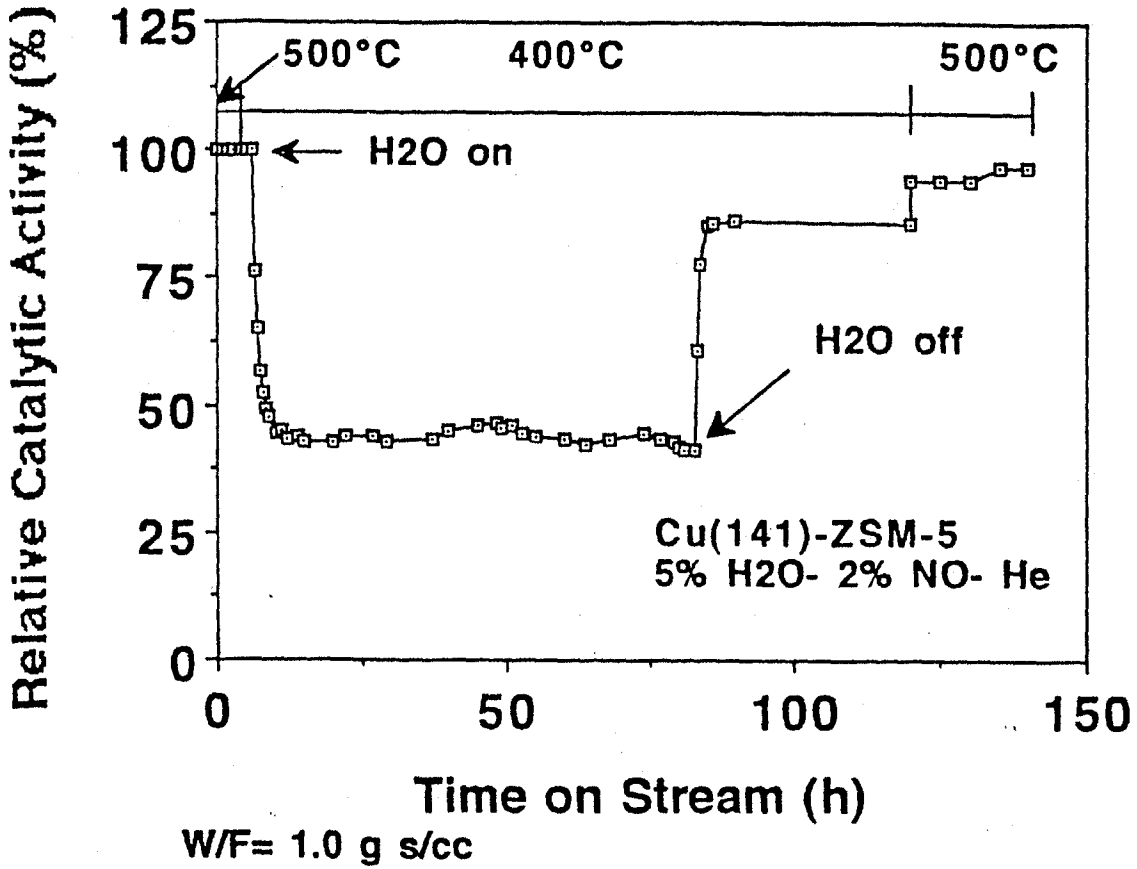

Figure 19. Effect of H2O vapor on the NO conversion to N2 over Cu(141)-ZSM-5 in 20% H2O - 2% NO - He at 400°C, W/F = 1 g s/cc (NTP).

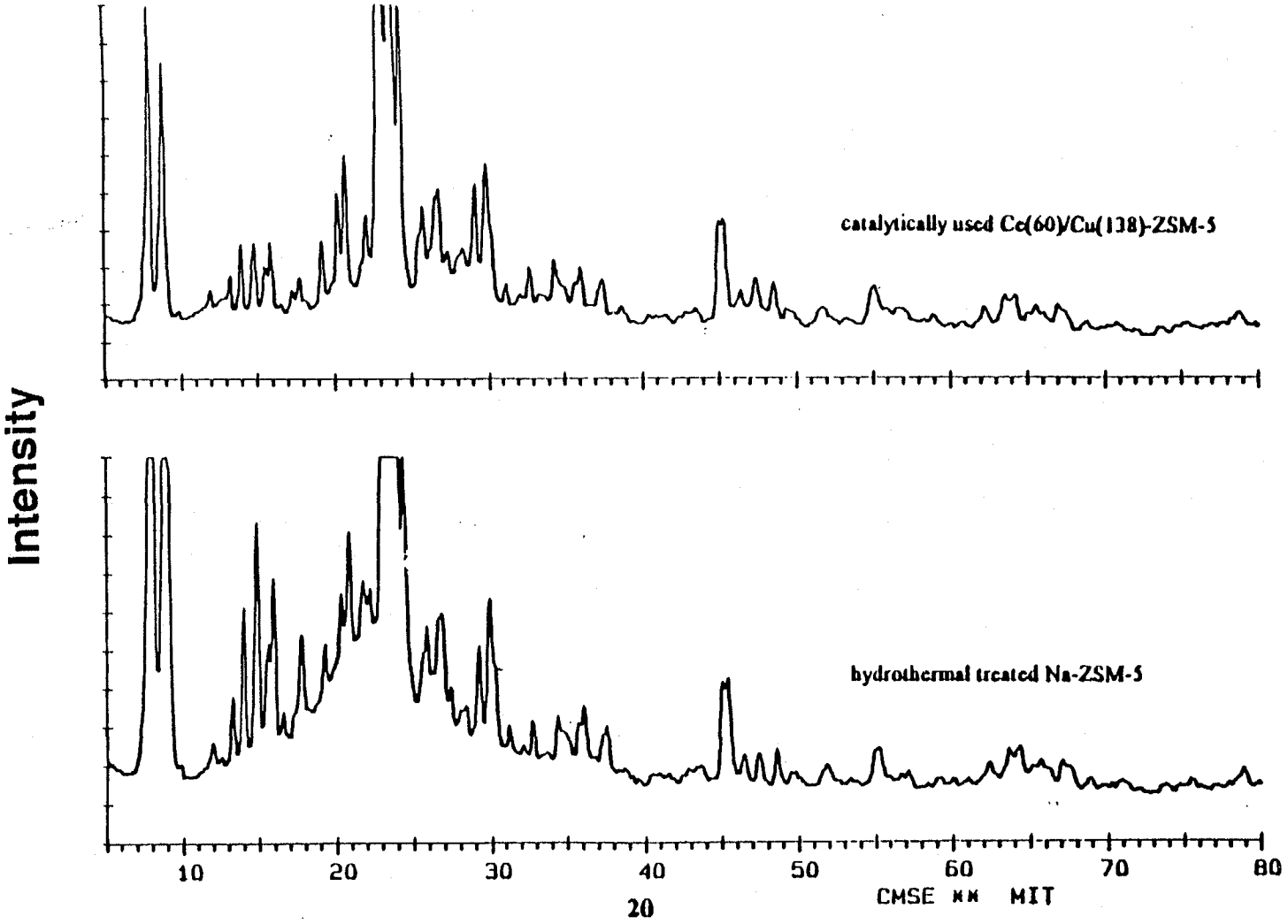

Figure 20. XRD patterns of the steamed Na-ZSM-5 (20 hours) in 20% H_2O- 4% O_2- He, and Cu(141)-ZSM-5, and Ce(60)/Cu(138)-ZSM-5 (10 hours) in 20% H_2O- 2% NO- He at 500°C.

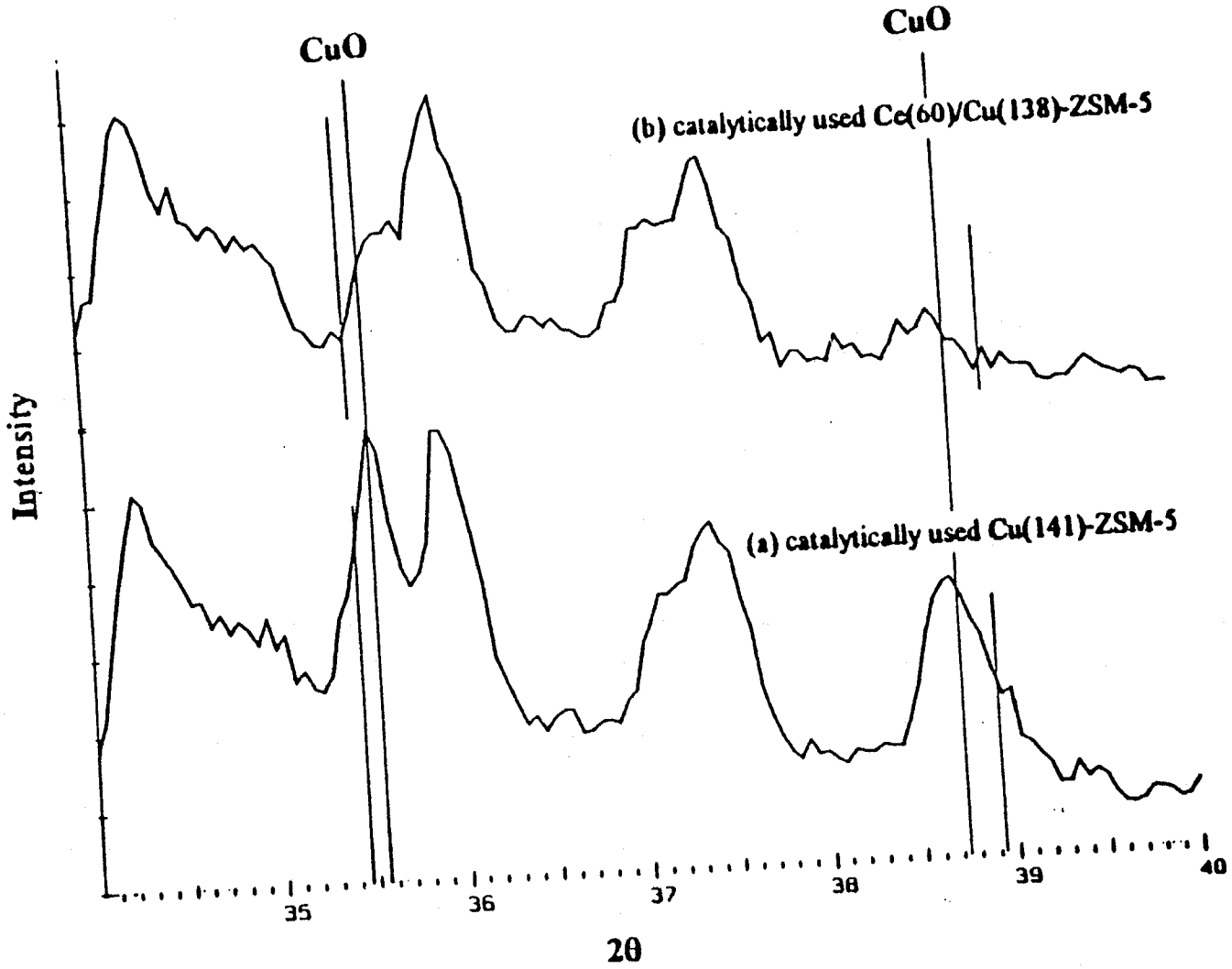

Figure 21. XRD patterns of (a) catalytically used Cu(141)-ZSM-5; (b) catalytically used Ce(60)/Cu(138)-ZSM-5 in both 20% H2O- 2% NO- He for 10 hours, then in 2% NO -He at 500°C for 20 hours.

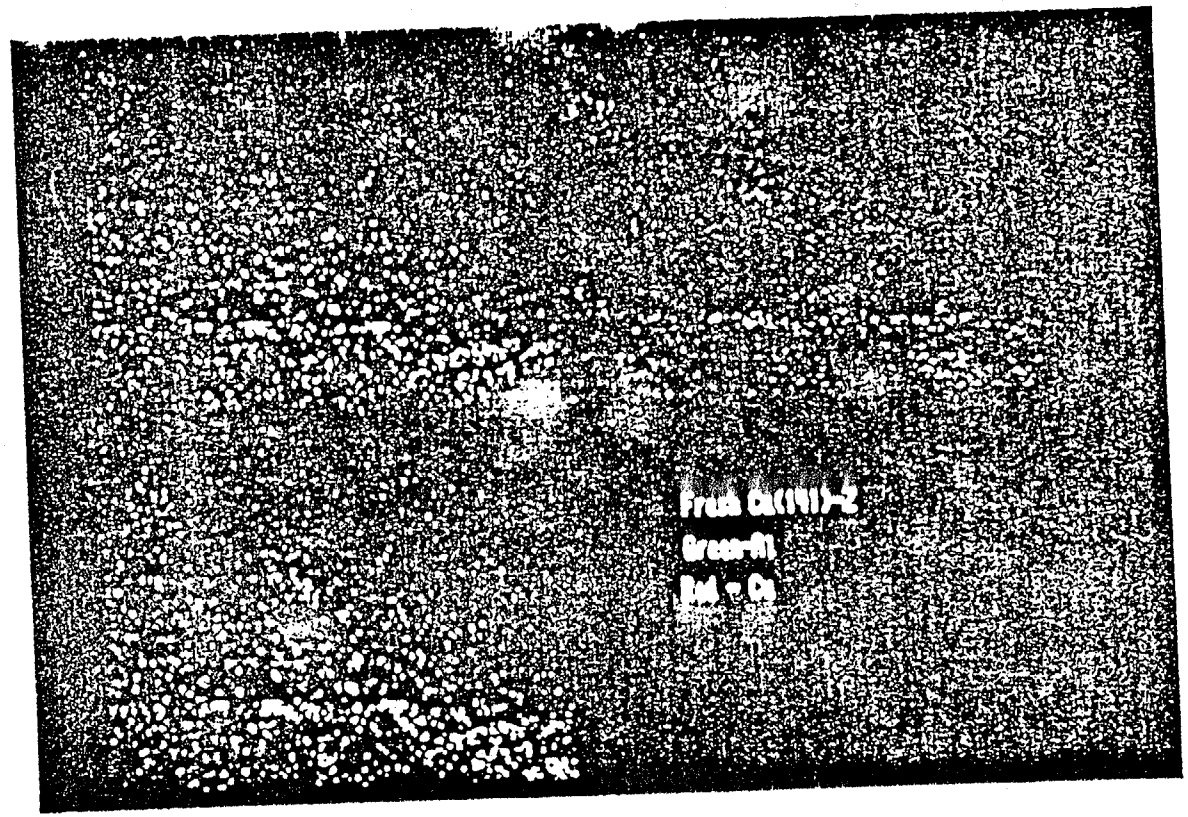

Figure 22. STEM/EDX mapping of Al and Cu cations in Cu(141)-ZSM-5 (a) 500°C- 2h. air calcined fresh sample; (b) catalytically used sample in 20% H2O - 2% NO -He for 10 hours, in 2% NO -He at 500°C for 20 hours (scale of a mapping: 100 nm by 120 nm).

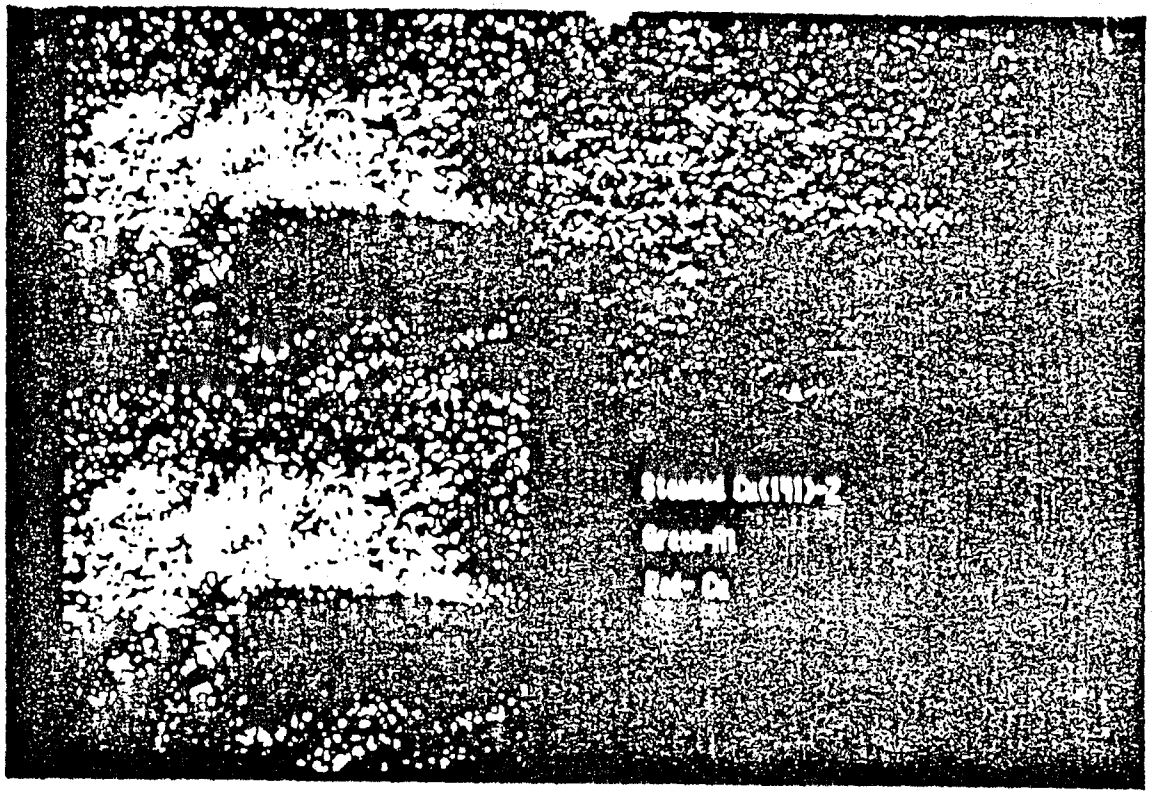

Figure 22b

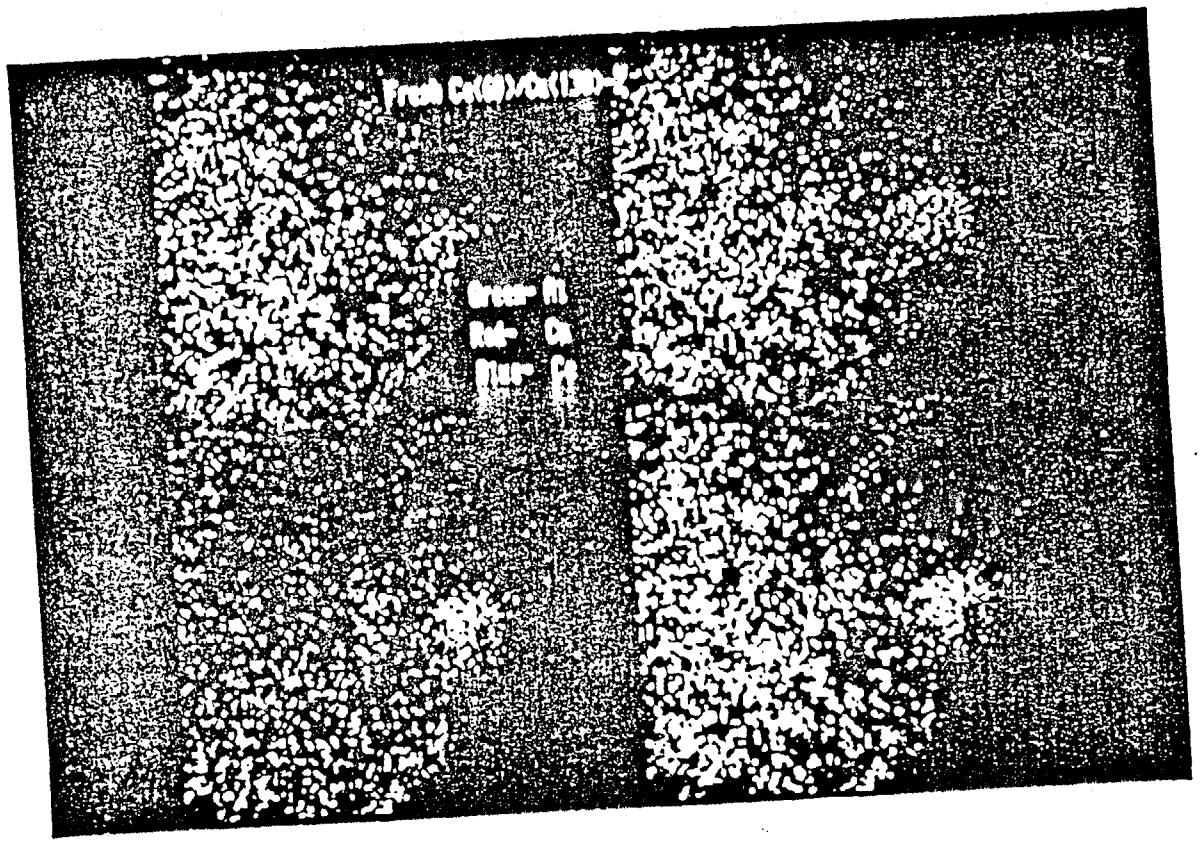

Figure 23. STEM/EDX mapping of Al, Cu, and Ce cations in Ce(60)/Cu(138)-ZSM-5 (a) calcined fresh sample; (b) used in 20% H2O- 2% NO- He at 500°C for 10 hours; (c) used in 20% H2O- 2% NO- He for 10 hours, then in dry gas (2% NO- He) for 20 hours at 500°C.

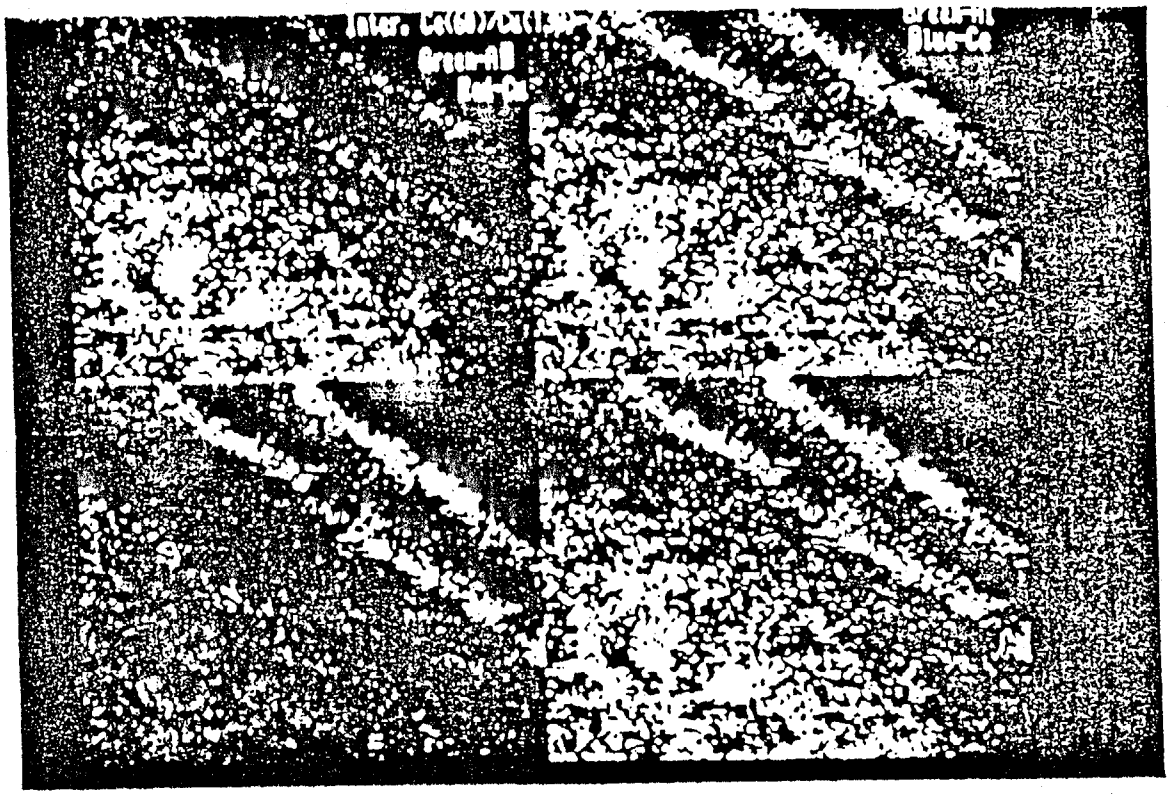

Figure 23b

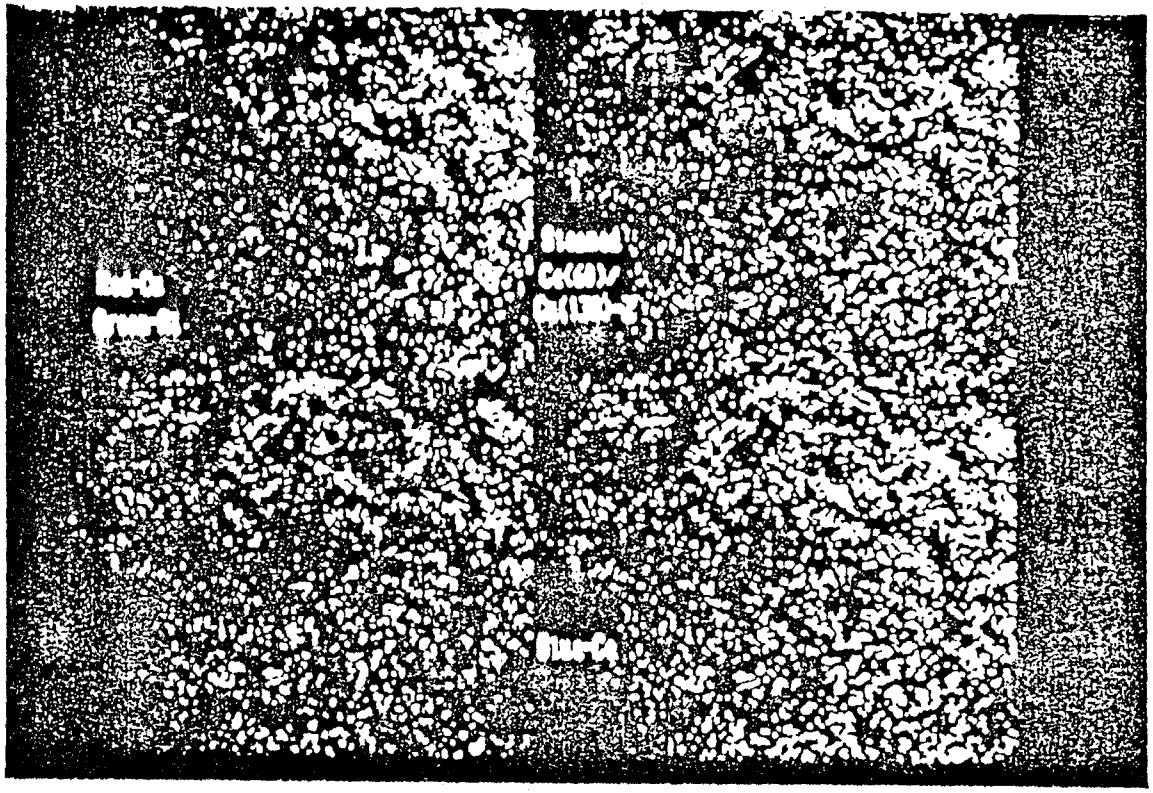

Figure 23c

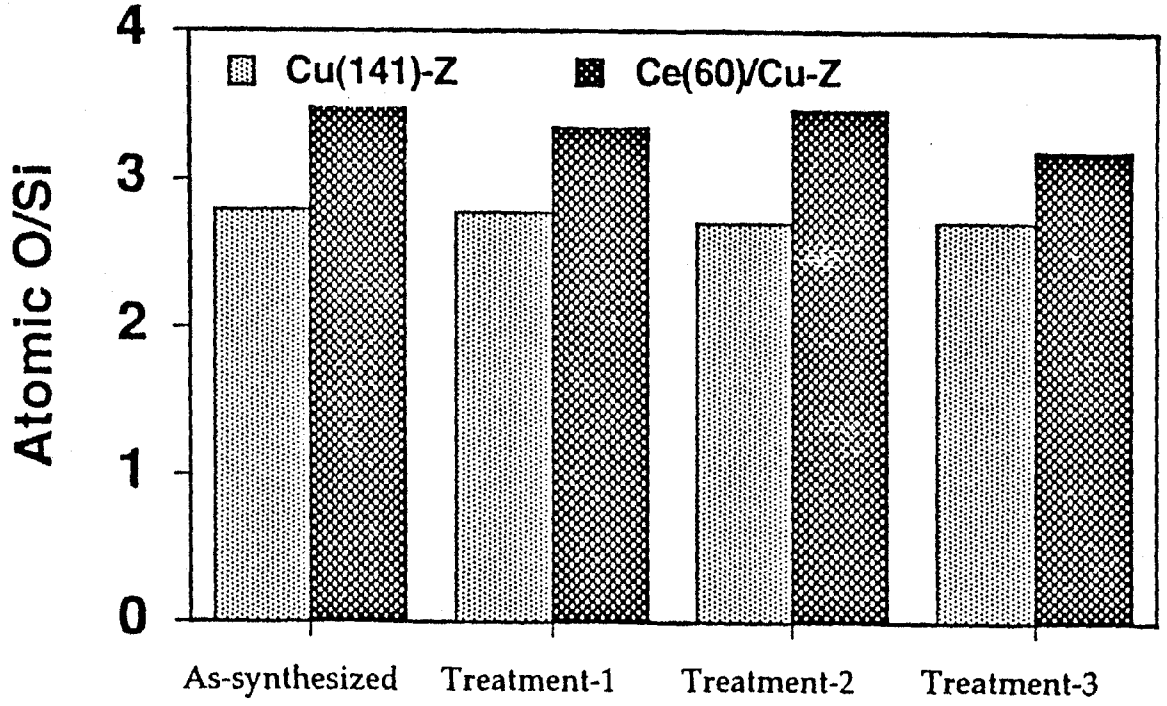

Figure 24. Atomic O/Si of Cu(141)-ZSM-5 and Ce(60)/Cu(138)-ZSM-5 measured by XPS (300 W, 15 KV; pass energy: 178 eV); fresh: uncalcined; treatments: (1) in He for 2 hours, then in 2% NO - He at 500°C for hours; (2) in 20% H_2O - 2% NO - He at 500°C for 10 hours following the first treatment; (3) in 2% NO - He at 500°C for 20 hours following treatment-2.

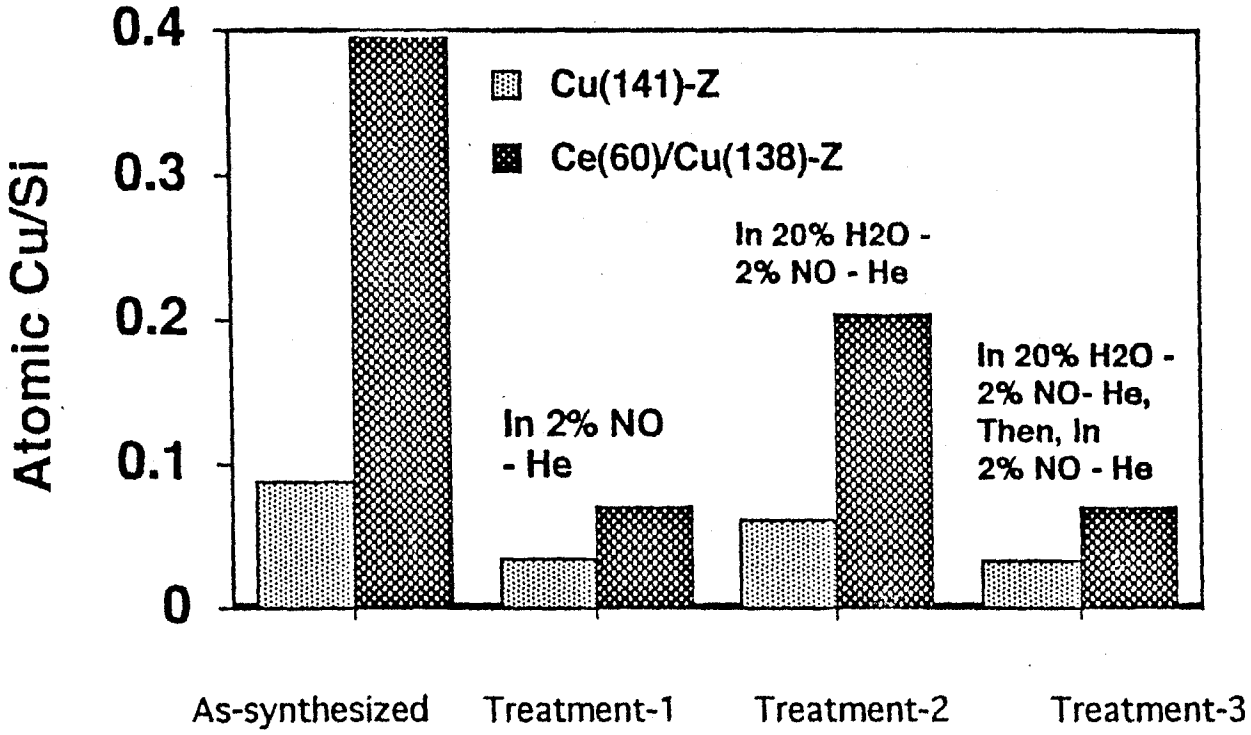

Figure 25. Atomic Cu/Si of Cu(141)-ZSM-5 and Ce(60)/Cu(138)-ZSM-5 measured by XPS (300 W, 15 KV; pass energy: 178 eV); fresh: uncalcined; treatments: (1) in He for 2 hours, then in 2% NO - He at 500°C for hours; (2) in 20% H_2O - 2% NO - He at 500°C for 10 hours following the first treatment; (3) in 2% NO - He at 500°C for 20 hours following treatment-2.

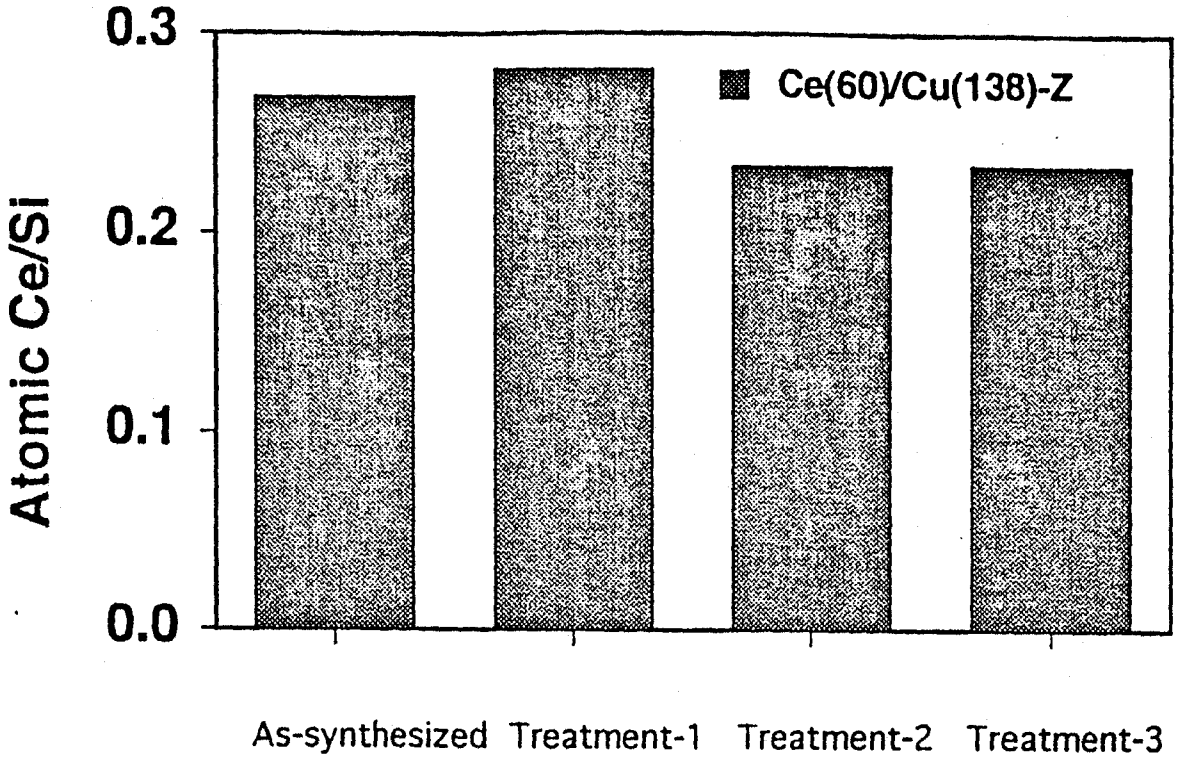

Figure 26. Atomic Ce/Si of Ce(60)/Cu(138)-ZSM-5 measured by XPS (300 W, 15 KV; pass energy: 178 eV); fresh: uncalcined; treatments: (1) in He for 2 hours, then in 2% NO - He at 500°C for hours; (2) in 20% H_2O - 2% NO - He at 500°C for 10 hours following the first treatment; (3) in 2% NO - He at 500°C for 20 hours following treatment-2.

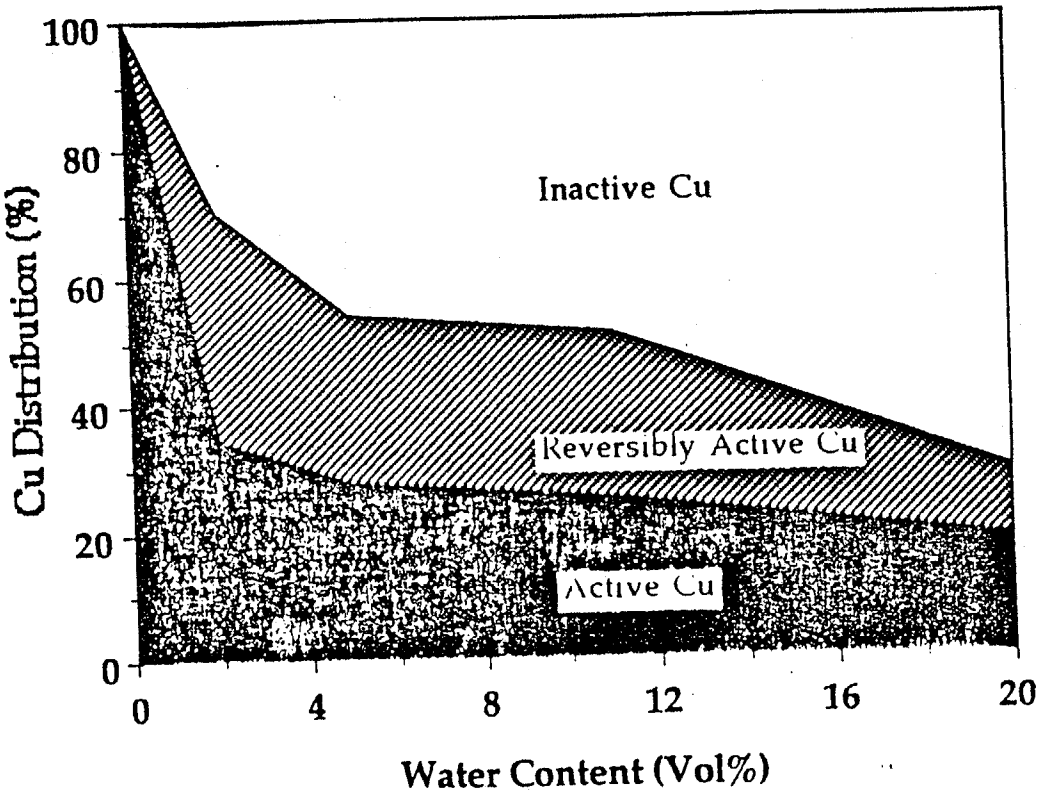

Figure 27. Estimated copper site distribution of Cu(141)-ZSM-5 in dry/wet NO decomposition in 2% NO- He, at W/F= 1.0 g s/cm3 (NTP) and 500°C.

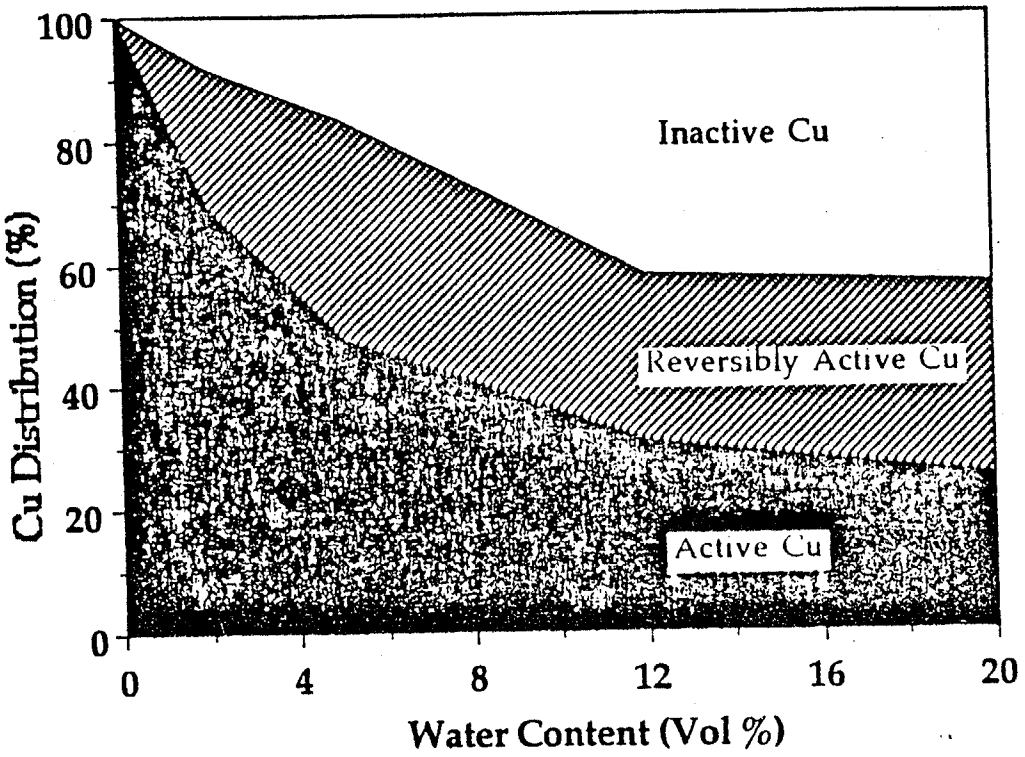

Figure 28. Estimated copper site distribution of Ce(60)/Cu(138)-ZSM-5 in dry/wet NO decomposition in 2% NO- He, at W/F=1.0 g s/cc (NTP) and 500°C.